TAMPEREEN TEKNILLINEN YLIOPISTO
TAMPERE UNIVERSITY OF TECHNOLOGY

SETAREH ZAKERI

# IMPACT OF DOPING AGENT AND PROCESSING PARAMETERS ON SPRAY DRYING THE ALUMINA NANOCOMPOSITE COLLOIDAL SUSPENSIONS

Master of Science Thesis

Examiners: Prof. Erkki Levänen
Prof. Mika Valden
Doctoral Student Amandeep Singh
Examiners and topic approved by the
Faculty Council of the Faculty of
Engineering Sciences
on 9th of November 2016

# ABSTRACT

**SETAREH ZAKERI**: IMPACT OF DOPING AGENT AND PROCESSING PARAMETERS ON SPRAY DRYING THE ALUMINA NANOCOMPOSITE COLLOIDAL SUSPENSIONS
Tampere University of Technology
Master of Science Thesis, 65 pages
Nov 2016
Master's Degree Programme in Science and Bioengineering
Major: Nanotechnology
Examiners: Prof. Erkki Levänen
Prof. Mika Valden
Doctoral Student Amandeep Singh
Keywords: Spray drying, Colloidal suspensions, Alumina, Graphene oxide, Solid spherical granules, Rheology.

This thesis was mainly concentrated on achieving the optimized formulation of doped and un-doped alumina suspensions in order to obtain spray-dried granules with the highest solid content, solid spherical morphology and narrow size distribution. The impact of the primary particle size (0.3, 0.6 and 1 $\mu$m) and the added amount of doping agent (0.065 and 0.195 vol.%) on the optimized formulation of the suspensions were investigated. The results indicated that the solid content had to be decreased as the primary particle size was reduced. The highest solid content for the suspension of 1 $\mu$m powder was 70% (with 0.3 wt% dispersant) whereas, it reached to 50 wt% (with 0.2 wt% dispersant) for the suspension of 0.3 $\mu$m powder. Moreover, it was found that any solid content more than the optimized amount resulted into huge irregular, rod shaped and elongated structures whereas any dispersant amount more than the optimized amount ended into donut-shaped or spherical granules with the blow holes on their external surface.

The effect of doping agent, graphene oxide (GO), was clearly seen on increasing viscosity of the suspensions which resulted from the electrostatic interaction of negatively charged GO sheets and positively charged alumina particles. However, effect of GO on increasing the viscosity of the suspension for micron sized (1 $\mu$m) powder was not as strong as it was for the submicron sized powders. This effect was more pronounced when submicron sized primary particles (0.3, 0.6 $\mu$m) were used for the alumina suspensions. As a result of the increase in viscosity, 0.3 wt% dispersant was used for the doped suspensions of the submicron sized powder. Furthermore, 10 wt% reduction of solid content of the suspensions was required when the added amount of GO was increased from 0.065 vol.% to 0.195 vol.%.

# PREFACE

It was a great opportunity for me to work as a research assistant in the ceramic materials group of the Materials Science Department of Tampere University of Technology (TUT) for more than a year and then start my thesis as a research project for Picodeon LTD Oy which is a Finnish disruptive innovations high-tech company providing thin film coating solutions.

I would like to thank my supervisor Prof. Erkki Levänen whose full trust in me always encouraged me to improve my capabilities during working with him. I have always received his full support and advisable discussions which were very helpful not only for my thesis but also for my work experience. I would also like to thank Dr. Jari Liimatainen for his financial support of this project. It meant a lot to me when he used to come from Oulu to Tampere for attending our monthly meetings to see the progress of the work. Moreover, I would like to acknowledge Amandeep Singh who is a doctoral student in the ceramic materials group. He spent a lot of time for me and guided me through every step of this work even though he was on vacation. I would also like to thank Prof. Mika Valden as my supervisor from the Department of Physics.

Many thanks to the people who helped me for my experiments and helped me how to improve my thesis: Leo Hyvärinen for teaching me how use the spray dryer, Matti Järveläinen for helping me to use the Dilatometer instrument and Sajjad Nouri for teaching me Latex and helping me in the writing part of my thesis.

In the end, I would like to thank my mom whose kind and warm words always gave me moral support. Although she was far from me, she helped me a lot to boost my morale.

*Tampere, Nov 2016*
*Setareh Zakeri*

# TABLE OF CONTENTS

# LIST OF FIGURES

# LIST OF TABLES

# LIST OF ABBREVIATIONS AND SYMBOLS

| | |
|---|---|
| 0D | Zero-dimensional |
| 1D | One-dimensional |
| 2D | Two-dimensional |
| 3D | Three-dimensional |
| $\alpha$ | Alpha (Transition aluminium oxide) |
| Al | Aluminum |
| $Al_2O_3$ | Aluminum oxide |
| $Al(OH)_3$ | Aluminum trihydroxide |
| Au | Gold |
| BET | Surface area ($m^2/g$) calculated by Brunauer-Emmet-Teller theory |
| °C | Celciuos |
| C | Carbon |
| $c_i$ | Concentration |
| cm | centimeter |
| CNT | Carbon Nano Tube |
| $CO_2$ | Carbon dioxide |
| cP | centiPoise |
| CVD | Chemical Vapor Deposition |
| $D_1$, $D_2$ | Size of the droplet |
| $d_{50}$ | Average particle size |
| $\delta$ | Delta (Transition aluminium oxide) |
| DAC | Dibasic Ammonium Citrate |
| $\eta$ | Eta (Transition aluminium oxide) |
| $\varepsilon_\circ$ | Permittivity of the air |
| $\varepsilon_r$ | Dielectric constant of the dispersion medium |
| EDS | energy-dispersive x-ray spectroscopy |
| F | Faraday constant |
| $Fe_2O_3$ | Iron oxide |
| $\gamma$ | Gamma (Shear rate) |
| g | gram |
| GO | Graphene Oxide |
| h | hour |
| $H_2$ | Hydrogen |
| $H_2O$ | Water |
| $H_2SO_4$ | Sulfuric acid |
| HCl | Hydrochloric acid |

| | |
|---|---|
| $HNO_3$ | Nitric acid |
| IEP | IsoElectric Point |
| $\frac{1}{K}$ | Double-layer thickness |
| $\kappa$ | Kappa (Transition aluminium oxide) |
| K | Kelvin |
| $KClO_3$ | Potassium chlorate |
| Kg | Kilogram |
| $KMnO_4$ | Potassium permanganate |
| kN | kiloNewton |
| kV | kiloVolt |
| m | meter |
| mm | millimeter |
| MPa | megapascal |
| mPa.s | millipascal-second terapascal |
| $\mu_1$, $\mu_2$ | Viscosity |
| $\mu$m | micrometer |
| MgO | Magnesium oxide |
| N | Newton |
| $Na_2O$ | Sodium oxide |
| $NH_3$ | Ammonia |
| $NH_4AlO(OH)HCO_3$ | Ammonium aluminum carbonate hydroxide |
| nm | nanometer |
| O | Oxygen |
| p | Probability level |
| $P_1$, $P_2$ | Nozzle pressure |
| PAA | PolyAcrylic Acid |
| PEG | PolyEthylene Glycol |
| $\pi$ | Pi |
| PMAA | PolyMethylAcrylic Acid |
| psi | Pounds per square inch |
| PVA | PolyVinyl Alcohol |
| PVP | Polyvinylpyrrolidone |
| R | Gas constant |
| rGO | reduced Graphene Oxide |
| rpm | rotation per minute |
| s | seconds |
| SEM | Scanning Electron Microscope |
| $SiO_2$ | Silicon dioxide |
| $SO_3$ | Sulfur trioxide |

| | |
|---|---|
| SPS | Spark Plasma Sintering |
| T | Absolute temperature |
| $TiO_2$ | Titanium dioxide |
| TPa | Tera Pascal |
| $\theta$ | Theta (Transition aluminium oxide) |
| V | Volt |
| Vol.% | Volume percent |
| W | Watt |
| wt% | Weight percent |
| $\chi$ | Chi (Transition aluminium oxide) |
| YAG | Yttrium-Aluminum-Garnet |
| $Z_i$ | Charge of counterions in the dispersion medium |
| $ZrO_2$ | Zirconium dioxide |

# 1. INTRODUCTION

Spray drying is a ubiquitous process involved in many industrial sectors which is employed to fabricate engineered powders by transforming the liquid feedstock into the dried particulates in a single step [1]. The first patented design of this perpetual technique was registered in United States in 1872. Thus far, spray drying has undergone several design modifications which made this technique as an industrial-friendly method. The main principle of this method is based on convection mode in which the moisture is removed by spraying the liquid feedstock into a hot drying medium [2]. This continuous particle-processing drying technique is capable of using different feed types such as solutions, suspensions, emulsions and dispersions. Depending on the chemical and physical characteristics of the feed and the design of the dryer, the spray-dried product can be achieved in different forms such as powders, granules or agglomerates [3].

Spray drying is known to be a superior technique compared to other liquid drying methods due to its high productivity of flowing powders with specific particle size, its capacity to handle varied nature of raw materials and its wide range of applications. This technique is implemented in food industry in order to produce whey powder, infant food, coffee/tea whitener, casein, encapsulated flavors, etc. In addition to food applications of spray drying, it has been used in other fields as well for producing detergents, pigments, fertilizers, antibiotics, vitamins, vaccines, enzymes, ceramic materials, etc [2].

In ceramic industry, the powder compaction process is commonly used as a shaping technique for ceramic materials due to its low cost and high productivity. However, this technique suffers from the density gradient which is originated during filling the die and the subsequent compression process since most of the technical ceramic powders are in range of one micron and do not flow very well [4], [5]. Thus, it is necessary to produce granules in the range of 100 microns which flow well and slide on each other during the die cavity filling [5]. This guarantees to achieve products with high homogeneity of the green density which is required for the high quality and less microstructural defects of the sintered body [4].

In ceramic industry, spray drying is considered as the most efficient method to convert ceramic suspensions into free-flowing ceramic powders. The main purpose of the implementation of spray drying in ceramic industry is to produce powders which can be homogenously compacted and then sintered. It is believed that narrow size distribution and spherical particle morphology are the main requirements to increase the flowability of the spray-dried powder and the die fill density. However, several parameters are strongly involved in order to obtain narrow size distribution of solid spherical granules with good compressibility behavior [6]. These parameters can be divided into two categories: operational parameters involved in the spray drying system and formulation of the prepared suspension for spray drying.

Spray drying has been widely employed for the fabrication of advanced ceramics such as, borides, nitrides, carbides and aluminas [6]. Among the ceramic materials, alumina is considered as the most well-known and most commonly used oxide ceramic powder due to its unique properties such as chemical stability, oxidation resistance, high electrical and thermal insulation, good mechanical properties and low production cost. The aforementioned properties of alumina have made this ceramic material applicable in the various fields [7], [8]. However, the applications of alumina are limited due to its brittleness and intrinsic low fracture toughness which implies the resistance of the structure to the formation of crack and its propagation [7].

In order to remedy this shortcoming of alumina, secondary phases with higher fracture toughness and mechanical properties have been utilized in alumina matrices [8]. Among these secondary phases, the graphene-based ones are proved to increase the mechanical properties of alumina significantly. However, there are some challenges associated with the utilization of graphene as it has poor dispersibility in aqueous and non-aqueous solvents and is chemically inert. The effect of these two properties of graphene prevents the required strong interaction of graphene and the matrix and limits the homogeneous distribution of graphene. On the other hand, graphene oxide (GO) which can be readily achieved by the exfoliation of graphite oxide is known to be a better secondary phase for polymers, metals and ceramics due to its abundant functional groups and hydrophilic surface state [9].

Although recently there have been some researches aimed to fabricate graphene-based alumina nanocomposites, thus far, no work has been performed yet for the fabrication of the novel GO-alumina nanocomposites by means of spray drying. Therefore, the target of this master thesis is to achieve highly flowable granules of GO-alumina with narrow size distribution and solid spherical morphology in order to reduce the density gradient of the compressed green body and increase its homogeneity. The novel GO-alumina nanocomposites made from the compression of the

spray-dried granules with the aforementioned properties can be emerged as functional nanocomposites for various applications as both alumina and GO are extremely exciting materials with outstanding properties.

It should also be mentioned that despite all attempts for sintering the compressed green bodies by means of vacuum furnace, the instrument was crashed for some technical reasons and therefore, we had to downgrade the outlines of this thesis and exclude the hardness measurements, sintering behavior characterization and archimedean measurements of the sintered samples.

# 2. BACKGROUND REVIEW

This chapter is devoted to give detailed description of the main materials used in this study as well as the methods which were used for the aim of this research work. The aim of this master thesis is to prepare spherical spray-dried granules of alumina/graphene-oxide and fabricate novel nanocomposites through compaction of the granules and characterize properties of them. Therefore, it is worth to discuss about the main raw materials of this study which are alumina ($Al_2O_3$) and graphene oxide (GO).

## 2.1 Alumina

### 2.1.1 General properties

Advanced ceramics are produced by refined minerals or synthesized oxide powders such as $Al_2O_3$, $ZrO_2$, MgO, etc. Among these oxide ceramics, alumina is is the most commonly used one due to its abundance in nature, its diverse forms and unique properties. Generally, alumina molecules have high energetic ionic and covalent bonds which make it as one of the most chemically stable oxides under harsh conditions such as high temperatures or strong acidic or alkaline environments [10]. Other unique properties of alumina such as good mechanical properties, oxidation resistance, high electrical and thermal insulation and low production cost, have made alumina involved in many potential applications covering dental implants, wear resistance parts, fast speed cutting tools, chemical and electrical insulators and different coatings [7], [8].

Alumina is available in various phases such as $\alpha$, $\chi$, $\eta$, $\delta$, $\kappa$, $\theta$, $\gamma$ and $\rho$ depending on the crystalline structure differences [11]. Each of these phases have specific properties which make alumina applicable in wide range of applications. The $\alpha$-alumina is the most abundant phase of alumina in nature and is thermodynamically stable at high temperatures. Therefore, it can be employed as coatings in order to keep the surface of the materials safe from wear [12]. Alumina is formed from aluminum and oxygen atoms and is the final product of the thermal treatments of all the

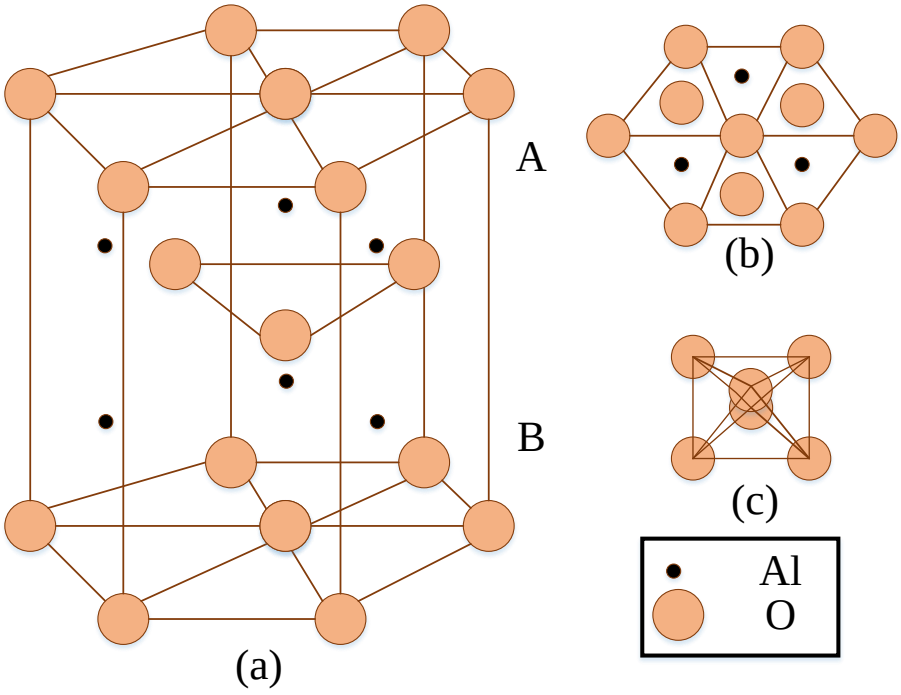


***Figure 2.1*** *(a) Corundum structure of α-alumina, (b) top view of this structure, (c) octahedral structure of α-alumina [11].*

aluminum hydroxides [11]. The polycrystalline $\alpha$-alumina with density of 3980 kg/m$^3$ and hexagonal structure is formed at high temperature above 1200 °C and the melting temperature for this phase is 2051 °C [13]. The other phases are named as so-called transition alumina phases which are formed during the thermal decomposition of aluminum hydroxides under various conditions. These metastable phases will be transformed to the $\alpha$ phase at specific temperatures whereas the $\alpha$ phase does not change into these phases as it is thermodynamically stable [11].

The crystal structure of the $\alpha$-alumina is shown in Figure 2.1. This structure is so-called corundum structure consisting of closed packed planes (plane A and B) of large oxygen anions with the radius of 0.14 nm being stacked in the sequence. According to the valence number of aluminum cations (+3) and oxygen anions (-2), for every three $O^{-2}$ ions only two $Al^{+3}$ ions are required in order to maintain electrical neutrality. Therefore, the aluminum cations with the radius of 0.053 nm occupy two-thirds of the octahedral sites of the basic array [11].

### 2.1.2 Alumina preparation

In order to employ alumina in the advanced ceramics manufacturing, typically sub micrometer size range powder with narrow size distribution is required. This requi-

rement is important due to the fact that it ensures fast and uniform sintering behavior which results into uniform and homogenous grain size in the final product [14]. There are many techniques available for the preparation of alumina with the required distribution and purity. The characteristics of the produced powder as well as the yield and production cost are different for each technique. These chemical production methods are mainly involved with extracting alumina from its impurities. The majority of produced alumina in the world is made from bauxite which is a metal ore consists of 45-60% alumina [15]. Bayer process is considered as the most common method to produce alumina. In this method, the bauxite ore is ground in ball mills with sodium hydroxide. The caustic aluminate solution containing soda is used to treat the crushed bauxite. Typically, the dissolution reaction is performed under pressure with the temperature range of 140-280 °C. Reaction of the caustic solution with the aluminum hydroxide leads to the separation of impurities through filtration and sedimentation, leaving a clear solution. When the hydroxides are precipitated, the alumina powders can be obtained by heat treatment at the transition temperature of the hydroxides [11].

The maximum purity of $\alpha$-alumina produced by the Bayer process is in the range of 99.6-99.9%. However, the electronic devices such as YAG (Yttrium-Aluminum-Garnet) and titanium sapphire laser devices require the purity of $\alpha$-alumina to be more than 99.99%. There are industrialized processes for manufacturing of highly pure $\alpha$-alumina in which the starting materials such as aluminum hydroxide and alum are calcined [11]. These available methods with the chemical reactions involved in them are briefly discussed as the following:

**a. Thermal Decomposition of Inorganic Aluminum Salts** Alumina can be fabricated by the thermal decomposition of several inorganic aluminum salts such as ammonium aluminum carbonate hydroxide ($NH_4AlO(OH)HCO_3$). In this method, the ion content and pH of the water solution have crucial experimental effect. The particle size of the produced alumina with this method cannot be smaller than 200 nm. However, researchers have been recently successful to obtain 60 nm average size of alumina powders by the heat treatment of the crushed powder obtained by thermal decomposition [16]. The main disadvantage of this process is the generation of impurities during crushing the powders. The reaction involved in this method is shown in Equation 2.1 [11].

$$2\,NH_4AlO(OH)HCO_3 \longrightarrow Al_2O_3 + 2\,NH_3 + 2\,CO_2 + 3\,H_2O \tag{2.1}$$

**b. Hydrolysis of Aluminum Alkoxides** In this method, first aluminum alkoxide has to be obtained by the reaction of the metallic aluminum and alcohol groups. Aluminum hydroxide which can be transformed into alumina powder after thermal treatment can be produced by the hydrolysis of aluminum alkoxide. The following equations represent the reactions involved in this method where R is the hydrocarbon radical [11]:

$$\mathrm{Al} + 3\,\mathrm{ROH} \longrightarrow \mathrm{Al(OR)_3} + \frac{3}{2}\mathrm{H_2} \quad (\textit{Alkoxide formation}) \tag{2.2}$$

$$\mathrm{Al(OR)_3} + 3\,\mathrm{H_2O} \longrightarrow \mathrm{Al(OH)_3} + 3\,\mathrm{ROH} \quad (\textit{Hydrolysis process}) \tag{2.3}$$

$$2\,\mathrm{Al(OH)_3} \longrightarrow \mathrm{Al_2O_3} + 3\,\mathrm{H_2O} \quad (\textit{Thermal process}) \tag{2.4}$$

**c. Chemical Vapor Deposition (CVD)** In this method, fine and homogenous mixture of $\alpha$- and $\gamma$-alumina powders with the particle size of 50 nm are produced by the reaction of the vaporized $\mathrm{AlCl_3}$ and water vapor (Equation 2.5) at high temperatures in the range of 750-900 °C. In order to increase the content of the produced $\alpha$-alumina, it is necessary to thermally treat the powder at temperatures above 1200 °C [11].

$$2\,\mathrm{AlCl_3} + 3\,\mathrm{H_2O} \longrightarrow \mathrm{Al_2O_3} + 6\,\mathrm{HCl} \tag{2.5}$$

**d. Thermal Decomposition of Ammonium Aluminum Sulfate** Ammonium aluminum sulfate (aluminum alum) can be used for manufacturing highly pure alumina powders. It is mainly refined by the successive recrystallization during the heat decomposition of this material. However, this method faces the problem of exclusion of $\mathrm{NH_3}$ and $\mathrm{SO_3}$ gases which are formed during the heat decomposition process expressed in Equation 2.6 [11].

$$2\,\mathrm{NH_4Al(SO_4)_2 \cdot 12\,H_2O} \longrightarrow \mathrm{Al_2O_3} + 2\,\mathrm{NH_3} + 4\,\mathrm{SO_2} + 25\,\mathrm{H_2}O + 2O_2 \tag{2.6}$$

## 2.2 Graphene-Oxide (GO)

As it was discussed in the previous section, alumina possesses unique features which make it applicable to be utilized in various fields. However, these applications are limited by alumina's brittleness, intrinsic low fracture toughness and fabrication difficulties. The most important property is fracture toughness which implies the resistance of the structure to crack formation and propagation [7]. Therefore, improving

strength, hardness and fracture toughness of alumina are crucial in order to broaden the application fields of this ceramic. Despite the advanced sintering techniques such as spark plasma sintering (SPS) which have been used for microstructural refinement in order to enhance the strength, toughness and hardness of alumina, another efficient approach is to introduce secondary phases to alumina matrix and fabricate alumina-based composites [8]. During the last decade, it was proved that graphene-based materials can be used as a secondary phase to overcome these shortcomings of alumnia. Among these materials, GO is a promising reinforcing agent due to its abundant reactive groups and hydrophilic nature. The properties, structure and preparation methods of GO are discussed in detail in the following sections.

### 2.2.1 History of GO and its properties

Carbon gets its original name from the Latin word "carbo" which means charcoal. In the modern world, carbon has been considered as one of the most desirable elements for various applications and fields. This element is known as an allotropic material which means that depending on its different structures, it can obtain varying properties. The well-known allotropic forms of carbon are diamond and graphite which are made from carbon atoms but with different arrangement of the atomic structures. Diamond is known as the hardest material ever and has excellent thermal conductivity. In addition to diamond, graphite which is very soft and in grey color has also high thermal and electrical conductivity. Graphite consists of multiple layers in which carbon atoms are arranged hexagonally in a honeycomb structure as shown in Figure 2.2 [17].

Each two-dimensional (2D) flat layer is called as graphene in which each carbon atom is covalently bonded to three other carbon atoms. Graphene sheets are connected to each other through the weak van der Waals bonds which determine the softness and self-lubricating properties of graphite [17].

In 1994, graphene was introduced by Boehm et al. as the building block or single car-bon layer of graphite structure [19]. It is not only the building block of the 3D bulk graphite but also 0D fullerenes and 1D nanotubes can be derived from 2D graphene [9]. However, there was not any feasible way to isolate graphene till 2004 when it was discovered for the first time by Geim and Novoselov through exfoliation of the bulk graphite [20]. Afterward, many efforts have been made to investigate the properties of this exciting material. It was found that graphene has enormous specific surface area ($\sim$2630 $m^2/g$) and therefore large aspect ratio, high intrinsic mobility ($\sim$200,000 $cm^2V^{-1}s^{-1}$), high thermal conductivity ($\sim$5000 $Wm^{-1}K^{-1}$), excellent optical transmittance ($\sim$97.7%) and unique mechanical and electrical properties [21].

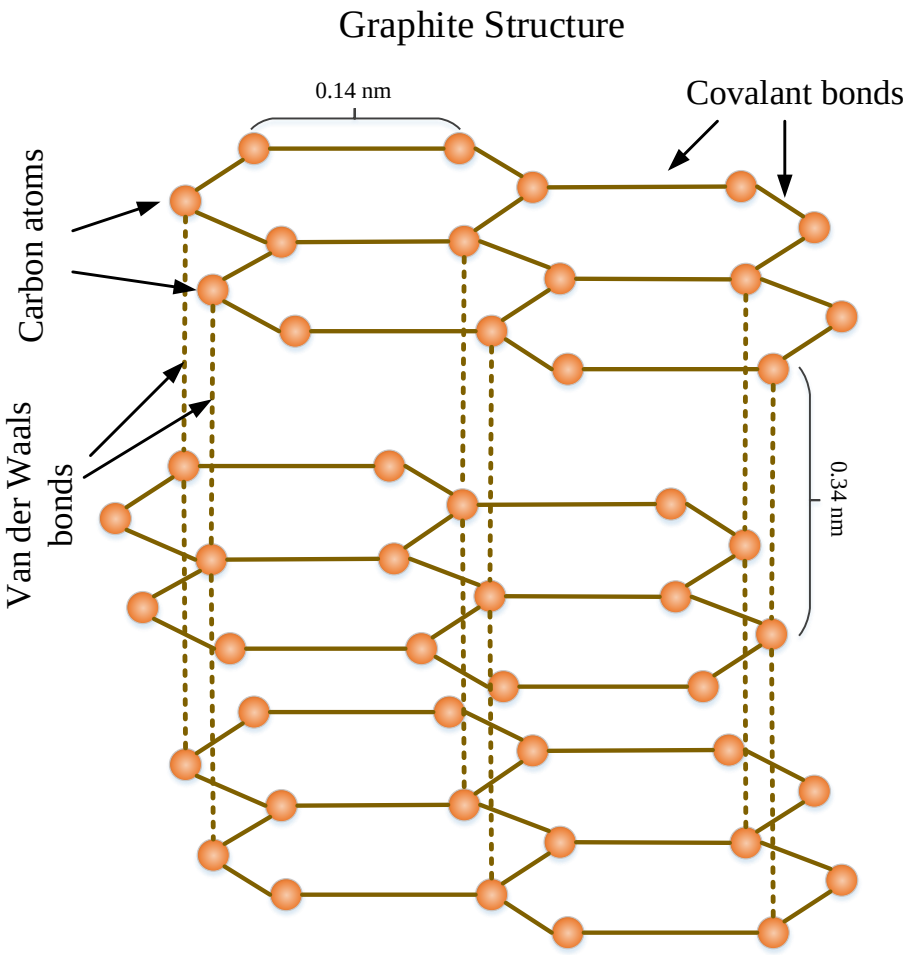


***Figure 2.2*** *Graphite structure [18].*

All these attributes have made graphene to be an ideal second phase for metals, ceramics and polymers in order to improve the aforementioned properties of them. These novel composites have been employed in several fields such as biosensors, super capacitors, lithium ion batteries and transparent conductors [22].

The high Young's modulus of graphene (∼1 TPa) is the main reason that makes it as a promising additive for reinforcing ceramic matrix composites [23]. Compared to conventional strengthening agents such as whiskers and fibers, graphene can induce smaller flaws and higher strength due to its nano-scale. In addition to that, graphene can be considered as lubricant since it reduces the friction force between the contact surfaces at both nano and micro scales. Only one layer of hard and strong graphene with nanometer thickness on ceramic grains is enough to improve the contact-damage resistance by working as lubricant [24].

In a study done by Porwal et al., $Al_2O_3$-graphene composites were synthesized and it was seen that the fracture toughness of alumina was enhanced up to 40% by adding

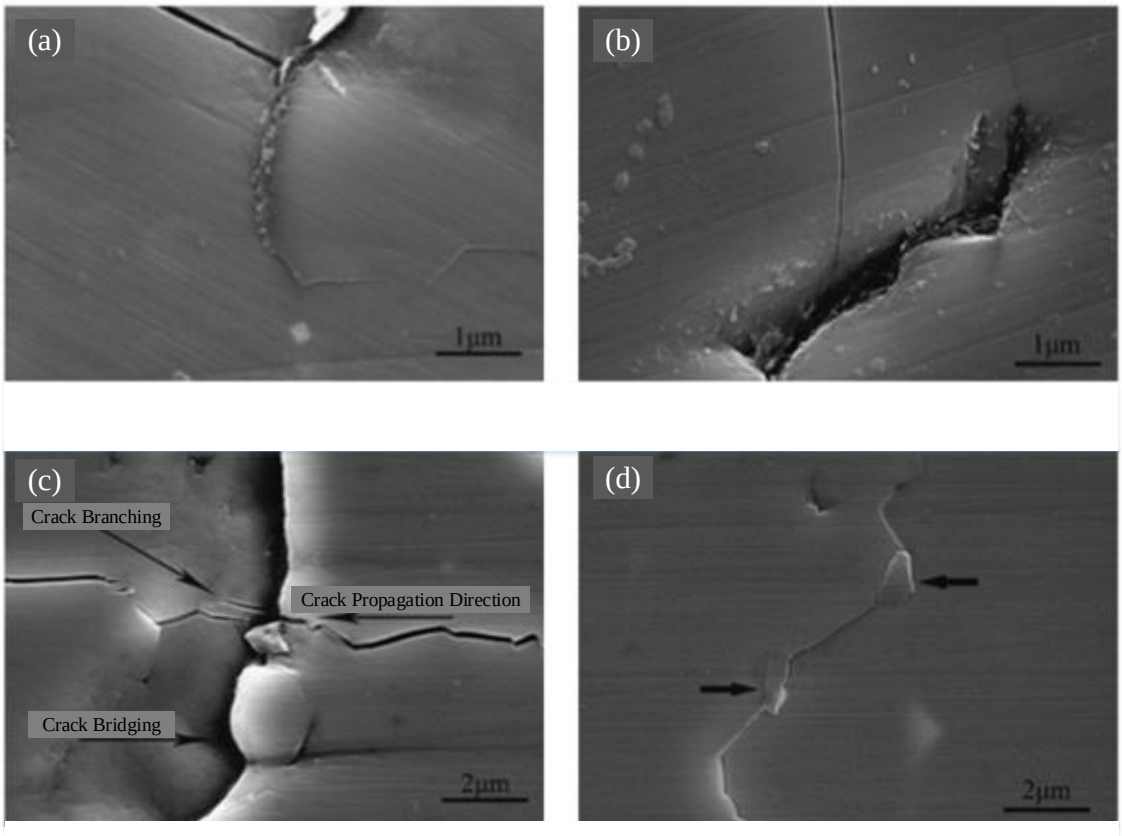


***Figure 2.3*** *Toughening mechanisms of graphene in alumina matrix: (a) crack deflection, (b) crack stopping, (c) crack bridging and (d) crack branching [25].*

only 0.8% graphene. This was explained by the fact that graphene was anchored in between the alumina grains and by making the crack paths more twisting and tortuous, it toughened the composites [22].

Several toughening mechanisms have been observed in $Al_2O_3$-graphene composites such as crack bridging, crack deflection, crack stopping and crack branching. Crack bridging happens when nanosheets dissipate fracture energy effectively whereas crack propagation stops when cracking is slowed down by the action of the graphene nanosheets. Crack branching is another toughening mechanism in which a crack is branched into several microcracks [25]. In addition to these mechanisms, crack deflection is enhanced by the large specific surface area of nanosheets. When these sheets which are along the alumina grains locate at the fracture surface, they will prevent in-plane propagation of the cracks leading to change in the propagation path and consequently to crack deflection [23]. The effect of these mechanisms are shown in Figure 2.3.

Two important parameters are required for the graphene to act as a reinforcing agent.

Firstly, the nanosheets must have good interfacial bonding to the matrix to transfer the load and improve the mechanical properties of the composites. Secondly, the distribution of the load throughout the nanosheets is required in order to guarantee that the most far away layers will not shear off. These requirements make graphene more favorable than carbon nano tubes (CNTs) for reinforced composites since due to the van der Waals forces between CNTs, they tend to form bundles and strong aggregations in the matrix [23].

However, there are some challenges associated with the utilization of graphene. Firstly, although graphite is available in large quantities and is considered as an inexpensive material, it does not exfoliate into monolayers of graphene sheets readily. Therefore, it is a major problem to produce graphene in large scale. Secondly, it has been always challenging to disperse and functionalize graphene due to its hydrophobic surface state and high chemical stability. Incorporation and homogenous distribution of graphene into various matrices are limited because of the strong C-C bonds available in the structure of the graphene. In order to overcome with this shortcoming, graphite oxide with its abundant oxygen-containing groups is a good solution since it can be easily obtained by the oxidation of graphite and it can be readily exfoliated to GO ans of the ultrasonic devices. GO, which has got the attention of the researchers, is the oxidized form of graphene and is a layered sheet material composed of oxygen-containing functional groups such as hydroxyl, carboxylic and epoxy groups on their basal planes and edges. In fact, GO is considered as the precursor for graphene (reduced GO) production through chemical and thermal reductions [9].

Due to the presence of the oxygenous groups, GO is more functionalized and more compatible with organic polymers. It is relatively hydrophilic and has great dispersibility in polar solvents such as water [26]. Unlike unoxidized graphene (without any oxidation and reduction treatments), GO and reduced graphene oxide (rGO) have more dangling atoms and functional groups which make it more efficiently bonded to the matrix. However they have less Young's modulus ($\sim$0.25 TPa for rGO) due to their more structural defects [24]. In recent years, much effort has been made in order to synthesize GO-derivatives such as GO-based nanoparticles, GO-based composites and GO-based coating and thin films [9]. GO films have been widely implemented in composite applications as a stiffening and strengthening additive [27].

### 2.2.2 GO preparation

The most common way of GO synthesis is through the chemical oxidation of graphite to graphite oxide accompanied by the subsequent exfoliation to achieve graphene

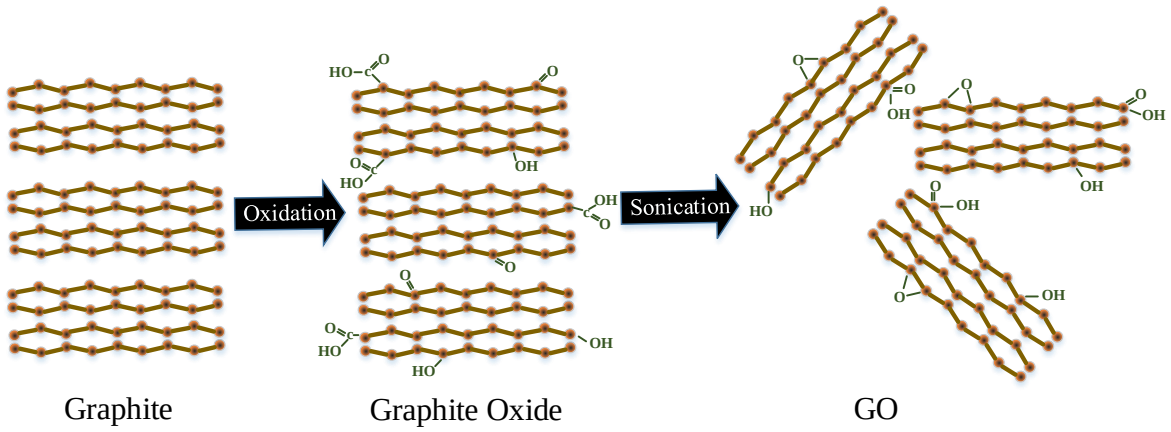


***Figure 2.4*** *Preparation of GO [9].*

oxide. This route can be divided into two steps as shown in Figure 2.4.

1. Oxidation of graphite powder into graphite oxide which can be dispersed in water easily due to the hydroxyl and epoxide groups at the basal planes and carbonyl and carboxyl groups at the edges of graphite oxide structure.

2. Exfoliation of the bulk graphite oxide by the sonication technique in order to achieve colloidal suspensions in which monolayer, bilayer or few-layer GO sheets are dispersed in various solvents [9].

Selection of appropriate oxidizing agents for oxidizing graphite is a crucial step in GO preparation. So far, different graphite oxide production methods such as Brodie, Staudenmaier and Hummers methods have been reported. In Brodie method, potassium chlorate ($KClO_3$) and nitric acid ($HNO_3$) are used to oxidize graphite whereas in Staudenmaier and Hummers method, sulfuric acid ($H_2SO_4$) and potassium permanganate ($KMnO_4$) are used, respectively. Although Brodie method is the most time consuming method, but the purest graphite oxide is obtained from this method whereas with the other methods possible contaminations due to the presence of sulfur and permanganate ions have been reported. Dispersed graphene oxide can be obtained by exfoliation of the graphite oxide dispersion by sonication [28].

The structure of GO, shown in Figure 2.5, consists of unoxidized benzene rings and regions with aliphatic six-membered rings which contain epoxy, hydroxyl, carbonyl and carboxyl groups [9]. According to the structure of GO, the present numerous reactive groups make it possible for GO to be functionalized with covalent and non-covalent bonds with other functional species to produce GO-based nanocomposites.

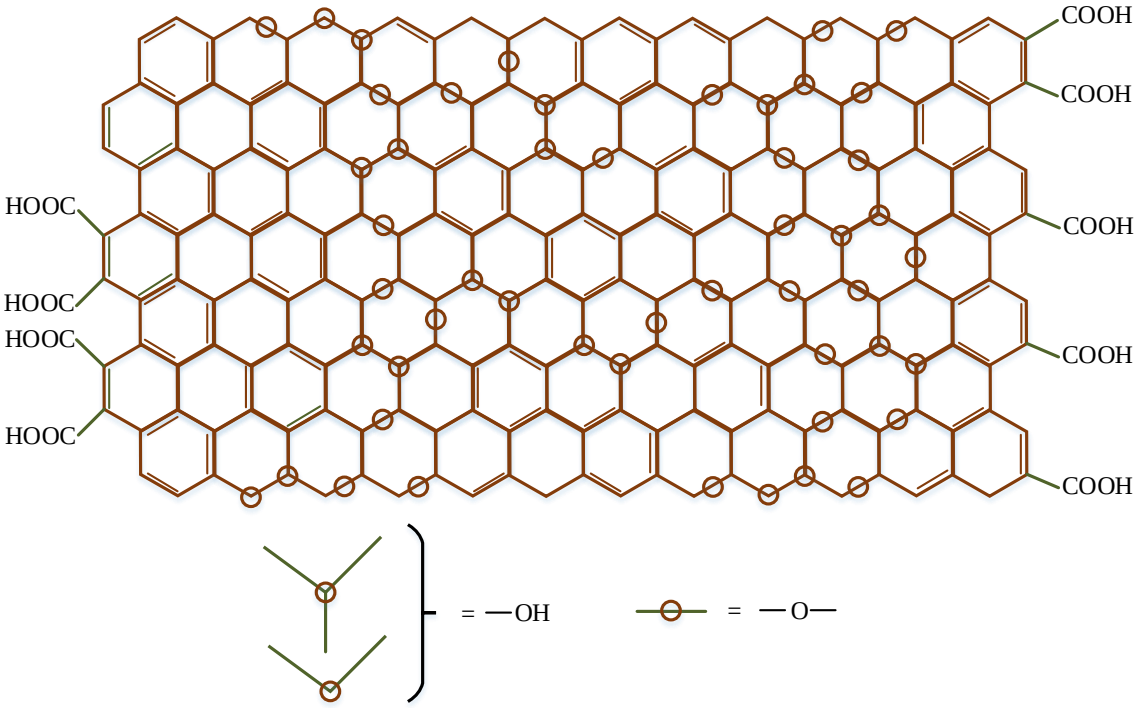


***Figure 2.5*** *Structure of GO [29].*

Non-covalent interactions of GO are mainly associated to the van der Waals interactions and $\pi - \pi$ stacking whereas covalent bonds are formed through the reactive groups by sharing electrons [9].

## 2.3 Granulation

Among the shaping methods in the industry of ceramics, the dry pressing is commonly used due to its lower production cost and high productivity compared to the wet forming techniques. The main requirement for this process is to use the free-flowing powders in order to ease the rapid die filling and also inhibit developing the packing defects [5]. Most of the ceramic powders used in the technical ceramics are in the range of one micron (fine powder) and do not flow perfectly. Therefore, granulation is a necessary step by which granules in the range of 100 microns are made from the primary fine particles [30]. Granulation is performed through a process called as spray drying in which an organic based or water suspension is sprayed into a hot medium. As a result of granulation, powders have better flowability, higher packing density and better compression behavior [31]. Any composite powder can be fabricated by aggregation of primary particles if a proper binder is used in the suspension [32].

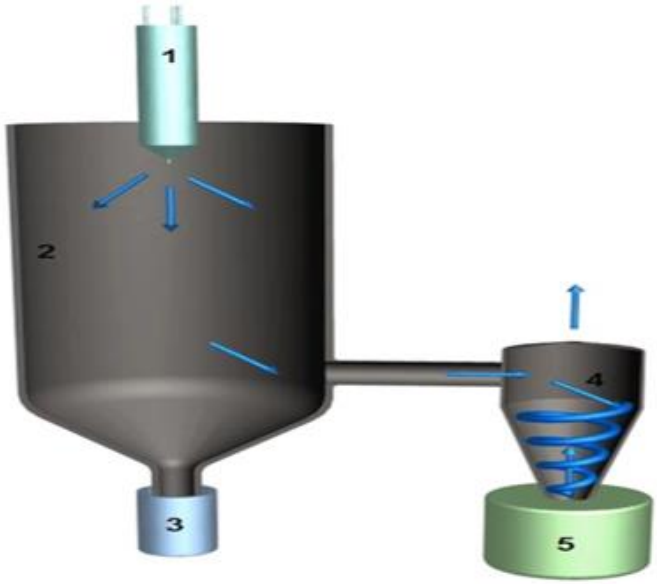


***Figure 2.6*** *Schematic diagram of a spray dryer: 1-spraying nuzzle; 2-drying chamber; 3-separation flask; 4-cyclone; 5-product vessel [34].*

### 2.3.1 Spray Drying

Spray drying is considered as one of the most versatile powder processing techniques by which a water-based suspension of powders (slurry) is atomized into a high temperature region and consequently due to the rapid heat and mass transfer granules are created [33]. The schematic diagram of a spray dryer is shown in Figure 2.6.

Once the slurry is atomized, the spray is introduced to the drying chamber to be in contact with the hot air and therefore, evaporation from the surface of the droplets is induced. The drying chamber which in most of the cases is filled with the heated gas is the place where granulation occurs [34]. Spray drying consists of four different stages:

1. Atomizing the suspension,
2. Contact of the droplets with the hot air,
3. Drying or evaporation,
4. Collecting the granules from the air.

Among all these four stages the atomization and drying steps are considered to be more effective on the final properties of the granules [35].

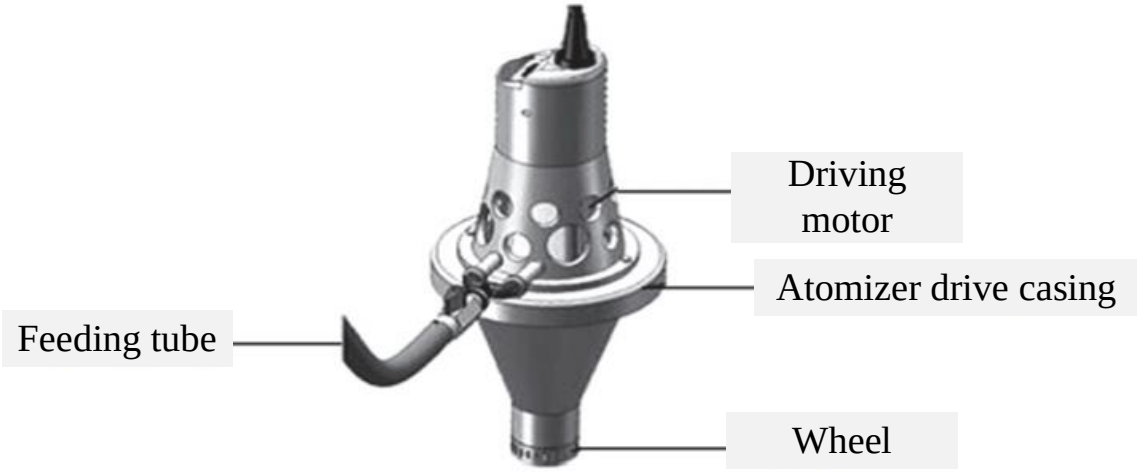


***Figure 2.7*** *Rotary nozzle [39].*

**Atomization**

Atomization is the main step in spray drying and the first transformation of the feed from the bulk liquid into a large number of droplets. The aim of this step is to provide an optimum spray for evaporation conditions in order to acquire the best economical products [36]. Typically, atomization of the liquid feed requires a force application. There are different atomizers available commercially which are categorized in accordance to the type of energy which generates the spray. The most common types of the atomizers are rotary atomizers (centrifugal energy) and pressure nozzles (pressure energy) [34] which are discussed as the following.

**1. Rotary Atomizer** This atomizer, shown in Figure 2.7, located in the ceiling of the drying chamber consists of a spinning wheel connected by a spindle and a gear with an electronic motor [37]. The feed is introduced to the spinning wheel or disk which rotates with high speeds up to 20,000 rpm from its center [38]. The slurry being pumped into the atomizer under low pressures (less than 100 psi), gets accelerated radially across the disc and then it is discharged from the periphery of the disc [39]. Droplets are formed because of the frictional forces between the drying air and the sprayed liquid and also the shear stress within the liquid [38].

The diameter of the disc varies from 40 cm for industrial size spray dryers to 5 cm for small laboratory spray dryers. The speed of the disc is in the range of 1000-50,000 rpm [40]. It is well proved that the mean droplet size is proportional to the feed rate, surface tension and viscosity whereas it is inversely proportional to the speed and diameter of the disc [2]. For this kind of atomizer, a large-diameter

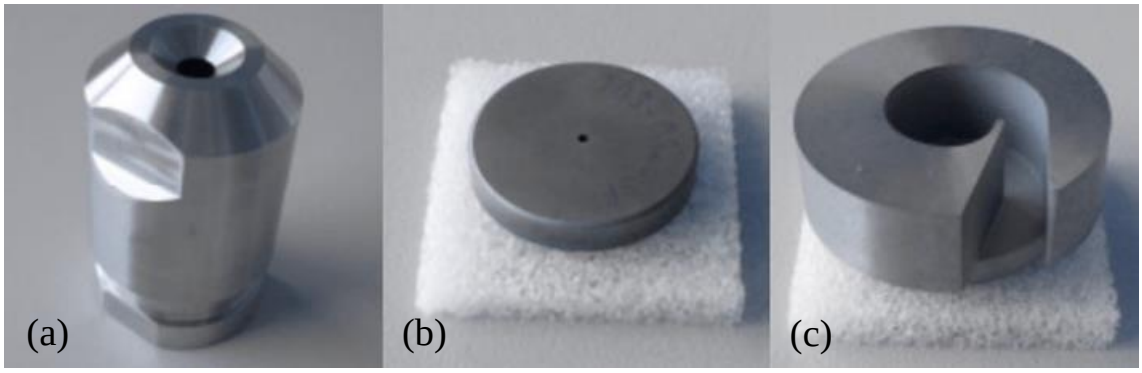


***Figure 2.8*** *(a) nozzle, (b) orifice plate, (c) swirl chamber [37].*

chamber is required since the droplets have high horizontal velocity. Although this type of atomizer is expensive and not suitable for very viscous slurries, it provides operational adjustments in the speed of rotating disc and the feed rate. The pumping system used for this atomizer is inexpensive because it feeds the slurry under low pressures [38].

**2. Pressure Nozzle** This type of atomizer, shown in Figure 2.8 (a), is very simple and comprises an orifice plate and a slot swirl chamber shown in Figure 2.8 (b) and (c), respectively [37]. The principle behind this atomizer is that the liquid feed is discharged from the orifice by the pressure energy which is converted to the kinetic energy and consequently the high speed film of feed will break into droplets. The droplets have high vertical speeds which necessitates the chamber to be long [2].

In order to pump the feed with this atomizer, high pressure up to several thousand psi, is required. Therefore, the pumping system is expensive whereas the nozzle itself is inexpensive. This nozzle is subject to wear as the slurry strikes the nozzle abrasively. As a result, a considerable variation in spray patterns are observed which will lead to the deposition of the droplets on the wall. The droplet size is proportional to the viscosity and surface tension of the feed whereas it is inversely proportional to the pressure [38].

### Contact of the droplets with hot air

Regarding to the stage of spray-air contact, subsequent to the atomization of the bulk feed to small-scale droplets, the droplets are brought into contact with hot air in order to evaporate the moisture from their surface. To achieve this target, uniform flow of gas through the drying chamber is required [2]. The drying time of

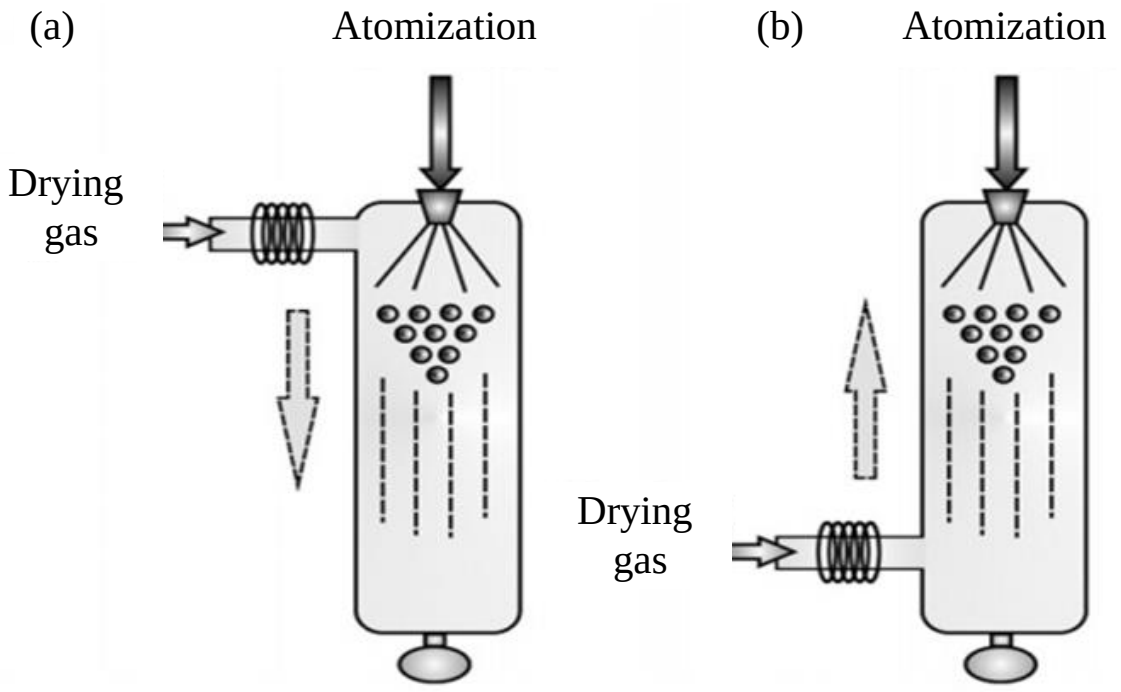


***Figure 2.9*** *Two different configuration of spray drier, (a) co-current and (b) counter-current [41].*

the droplets, their residence time and wall deposition in the chamber are dependent on the airflow pattern in the chamber. Practically, there are two configurations for the gas flow direction according to the position of the air disperser: co-current flow, counter-flow, which are depicted in Figure 2.9 [38].

In the co-current flow, the feed spray and the drying air go through the chamber in the same direction. In other words, the air inlet is positioned close to the atomizer. This configuration is commonly used in spray dryers equipped with rotary atomizers. In this case, the solvent gets evaporated rapidly since the residence time of the droplets is short otherwise the temperature of the granules will increase and their inherent properties might differ significantly [34]. The granules coming towards the bottom of the chamber will be in contact with the coolest air, so this design is more preferable for materials which are sensitive to heat. On the other hand, in the counter-current flow, the granules will be in contact with the hottest air where the spray and the air come from the opposite direction. Hence, it is not suitable for heat-sensitive materials [41].

### Drying or Evaporation

Once the droplets are exposed to the heated gas, the solvent gets evaporated until the moisture concentration becomes so low to migrate to the surface of the dried granule [36]. When the liquid is moving towards the outside of the droplet, the solid particles are also carried along. Consequently, when the heating rate is faster than the diffusion rate, a void can be created at the center of the droplet. Explosion is not preventable when the pressure inside the drop crosses a certain limit. Finally, when the solvent is lost, the final particle will be plasticized thanks to the presence of binder in the feed. The shrinkage of the particle due its surface tension will be stopped when the particle is completely dried [27].

The drying process is usually divided into two different phases: constant-rate drying and falling-rate drying. As the droplet, which consists of a considerable amount of liquid and free micro or nanoparticles in wet core regions, enters a heated medium, its temperature will increase up to the wet bulb temperature. The heat is transferred from the outer surface to the center by conduction [42]. This rise in temperature will be followed by the shrinkage of the droplet due to the evaporation from its surface. The shrinkage is shown as the first step depicted in Figure 2.10. This stage is called as constant-rate drying stage in which the temperature of the droplet is remained constant and equal to the wet bulb temperature. In this stage, the evaporation rate does not change since there would be a mass transfer of the liquid inside the droplet towards its surface and therefore, the droplet moisture changes steadily with time [2].

The droplet surface will be saturated at so-called ”locking point”, when the liquid concentration reaches to a minimum and subsequently a submerged agglomerated shell will be formed by the primary particles (step 2 in Figure 2.10). By further drying, a porous crust will be formed on the droplet surface and the first stage is ended. An additional resistance to evaporation is observed when a crust layer on the droplet surface is formed. The crust's thickness will be increased (step 3 in Figure 2.10) by the provided heat in the chamber and therefore the drying rate will decrease gradually [43]. This stage, known as the falling-rate drying, continues until a desired moisture is obtained. The droplet size in this stage is constant and equal to the final product size since the porous crust is expanding and the wet core is shrinking simultaneously. The water vapor diffuses through the pores of the crust layer [42]. Bubble formation is also observed in this stage when the pressure of the moisture vapor at the center of the droplet is higher than the ambient pressure and therefore a bubble is formed (step 4 in Figure 2.10). The temperature of the final product is assumed to be approximately 20 °C less than the outlet temperature [2].

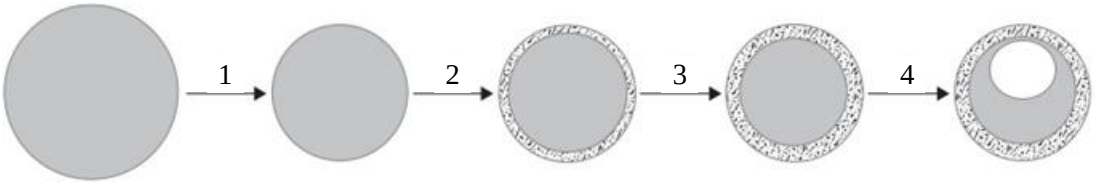


***Figure 2.10*** *Steps involved in drying the droplets inside the spray dryer chamber [2].*

**Granule collection**

The final spray-dried granules can be collected from separation flask and product vessel. Most of the granules are transported into the product vessel ans of a tube connecting the drying chamber and cyclone. The separation flask is positioned right beneath the drying chamber and is responsible for collecting the heavier and bigger granules. On the other hand, the finer particles are collected from the product vessel [44].

## 2.4 Effect of processing factors on the morphological properties of granules

An ideal size of the granules are believed to be in range of 50-100 $\mu$m. Moreover, the best morphology for the granules is the solid sphere since this shape can provide the granules with a higher flowability [5]. The dried granules could have variety of shapes: solid spheres, dimpled spheres, hollow spheres, needle-like, donut-shaped or elongated. The morphology of the obtained granules is strongly affected by several factors related to the operational conditions of the spray dryer such as the atomizer design, the temperature of the hot media and so forth [33]. In addition to that, the influence of the slurry formulation (dispersant, amount of binder, lubricant and etc.) is not negligible at all because the structure of the granules is strongly dependent on the dispersion state of the slurry [45]. Morphology is effective on several main characteristics of the product such as its flowability, size distribution, moisture content and density. Therefore, understanding the parameters which affect the morphological properties of the particles and also the most common patterns of morphology are required.

### 2.4.1 Atomization pressure

According to the Equation 2.7, when the atomization pressure is increased the size of the droplet will be diminished:

$$\frac{D_2}{D_1} = (\frac{P_2}{P_1})^{-0.3} \tag{2.7}$$

where $D_1$ and $D_2$ denote the size of the droplet when the nozzle pressure changes from $P_1$ to $P_2$ [2].

### 2.4.2 Atomization speed

The wheel speed is one of the most important and significant parameters affecting the granule size. By keeping the feed rate and wheel diameter constant, it has been well proved that with higher wheel speeds smaller particles can be obtained. In the performed experimental work [47], three different atomizer speeds (10,000, 11,000 and 12,000 rpm) were chosen to spray-dry milk into powder. Results revealed that that by increasing the atomizer speed, the average size of the spray-dried powders was significantly diminished ($p < 0.05$), however the chemical properties remained unchanged [47]. A research group investigated the effect of two functional variables: inlet temperature (190, 220 and 250 °C) and atomizer speed (18,000, 22,000 and 26,000 rpm) [48]. Results of this experimental work showed that by increasing the inlet temperature and atomization speed, the bulk density of the powder was decreased. In addition to that, it was observed that the particle size was increased by decreasing the atomization speed and it ranged from 1 to 60 micron depending on the different speeds used in their work.

### 2.4.3 Feed rate

By keeping the atomization pressure constant, the size of the droplet increases as the flow rate increases due to the fact that more liquid has to be atomized by the hydraulic energy of the nozzle. In this case, the interaction of the feed with the atomization energy is minimal hence, the droplets do not have enough energy to reduce their size. Some studies have been devoted to evaluate the effect of the feed rate. For example, one study has stated that higher flowability and smaller particle size can be obtained by low feed rate [49]. In another research work, the spray-dried microparticles showed slower drug dissolution rate and it was due to the large particle size produced by high feed rate [50].

### 2.4.4 Outlet temperature

The temperature of the air coming with the granules right before going through the cyclone is known as the outlet temperature. The outlet temperature is very

effective on the morphological properties of the product such as density, moisture level, granule size, particle shape and also roughness. Several authors have evaluated the effect of the outlet temperature on the morphology of the spray-dried powders. For instance, Paramita et al. have concluded that the percentage of hollow granules is higher when high outlet temperature is provided for the spray drying system [51]. In another study done by Mass et al., a solution was prepared for spray drying and three outlet temperatures (60, 90 and 120 °C) were selected to examine their effect. It was seen that by the lowest temperature, more spherical particles were formed whereas with the other temperatures void or hole formation was observed. This can be elucidated by the fact that when 60 °C is chosen for the outlet temperature, the internal pressure caused by the evaporating liquid is low enough to give the vapor proper time to escape without fracturing the shell and forming a void [52].

### 2.4.5 Inlet temperature

The inlet temperature is known as the temperature of the hot drying gas. The higher the inlet temperature, the quicker is the moisture content removal. However, the physical and chemical properties of the product may be distorted by high inlet temperatures. Therefore, it should not be used for heat-sensitive materials. The recent findings from an experiment showed the effect of inlet temperature on the product properties [53]. Two inlet temperatures, 150 and 170 °C, were chosen for this purpose. A desired powder should have low moisture content and high bulk density. The result of the aforementioned work showed that the production yield was increased at the higher temperature, whereas bulk density and moisture content were both decreased.

## 2.5 Effect of slurry formulation on the morphological properties of granules

Although slurry preparation is not considered as a step in spray drying process, the effect of slurry's formulation on the spray drying operation and the final properties of the granules is not negligible. Several properties and characteristics of the slurry which have significant impacts on the process of spray drying will be discussed as the following.

### 2.5.1 Solid-loading

Most of the ceramics spray-dried powders are obtained from the water-based slurries in which the ceramic powders have to be dispersed well. A slurry which has high

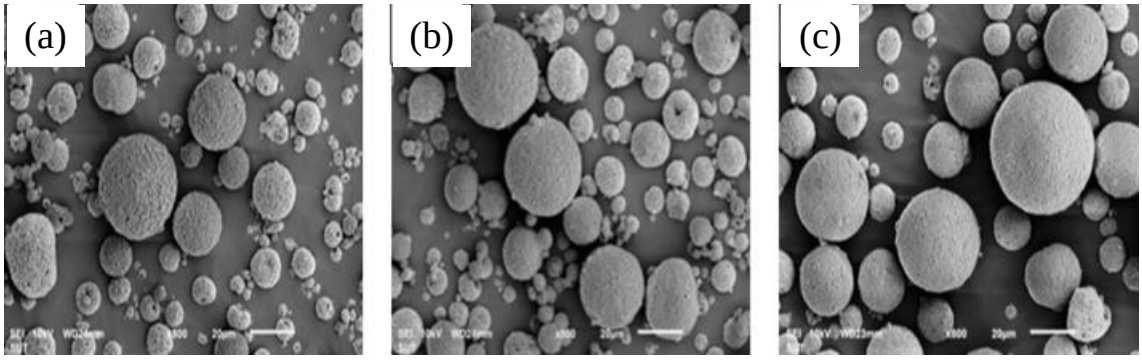


***Figure 2.11*** *Morphology of the spray-dried granules with (a) 50, (b) 60 and (c) 70 wt% solid-loading [54].*

solid-loading content is more favorable due to the technical and more importantly economic reasons. The solid-loading, weight percent (wt%), is measured by heating a small amount of the slurry up to a temperature sufficient enough to remove all the organics and water. When the water content of slurry is high, the water will finally be evaporated and therefore the powder yield is economically unfavorable. For instance, by increasing the solid-loading content from 50 wt% to 75 wt% the powder output will be tripled [38]. In another study done by Chiangka et al., effect of solid-loading on morphology of the spray-dried granules was investigated. Three different solid content of 50, 60 and 70 wt% composite slurries (90 wt% of alumina ($d_{50}$: 1$\mu$m) and 10 wt% of zirconia ($d_{50}$: 0.3$\mu$m)) were spray-dried. As shown in Figure 2.11, it was found that by increasing the solid content, the morphology of the granules was improved significantly in terms of having denser granules without internal holes or voids. The tap density and median size of the granules were increased by increasing the solid content. Spherical composite granules with uniform size distribution of $d_{50}$: 39.7$\mu$m were obtained by spray drying 70 wt% suspension [54].

In another research work implemented by Penbunditkul et al., the external and internal morphology of the spray-dried granules from bergamont oil emulsion with different solid concentrations (10, 20, 30 and 40 wt%) were examined. It was shown that the particle size was proportional to the solid concentrations and the external surface of the granules from higher solid concentrations (30 and 40 wt%) was smoother as shown in Figure 2.12 [55].

Another experimental study done by Bian et al. presented the preparation of four composite slurries (87 wt% $Al_2O_3$ and 13 wt% $TiO_2$ with grain size of 20-45 and 20-50 nm, respectively and polyvinyl alcohol (PVA) as binder) with different water content of 47, 55, 60 and 70 wt%. It was shown that the tap density and flowability of the spray-dried granules were decreased by increasing the water content of slurry.

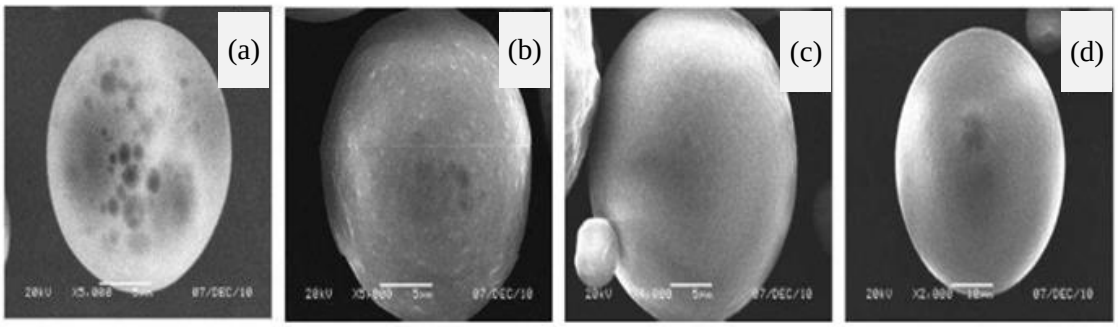


***Figure 2.12*** *External surface of spray-dried granule with (a) 10, (b) 20, (c) 30, (d) 40 wt% of solid-loading [55].*

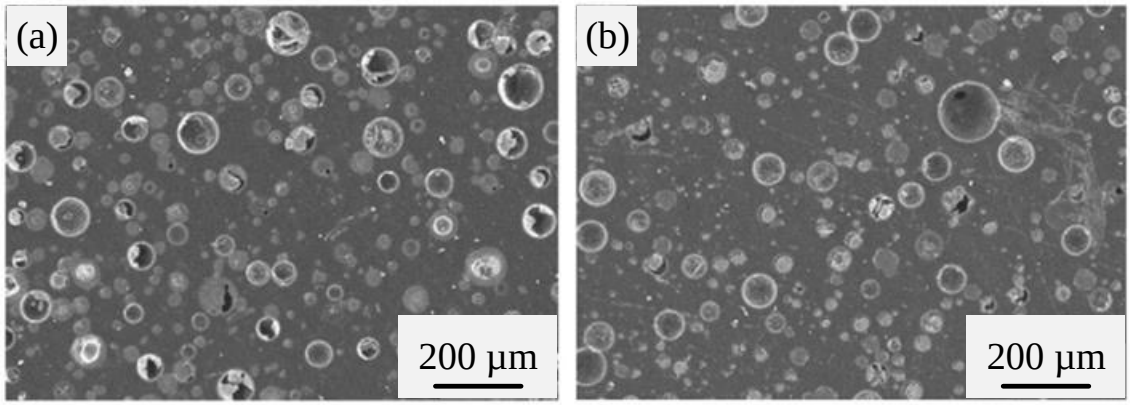


***Figure 2.13*** *Internal structure of the spray-dried granules with (a) 47 and (b) 70 wt% water content [56].*

The granules were spherical but some of the large particles had hollow structure as shown in Figure 2.13. Denser granules were achieved with the slurry with less water content (47 wt%) compared to the slurry with 70 wt% water content [56].

In the study of Sanchez et al., two composite slurries ($Al_2O_3$ (size: 10-20 nm)-13 wt% $TiO_2$ (size: 20-30 nm)) with 10 vol.% and 15 vol.% were prepared. The suspensions were dispersed by 4 wt% of polyacrylic dispersant. It was seen that many of the granules possessed donut-shaped morphology however granules from slurry with 15 vol.% had more spherical structure and narrower size distribution [57]. In another study, slurries with different solid-loadings from 25.5 to 51 vol.% were used for spray drying [5]. It was observed that by increasing the feed material solid-loading, the flowability and tap density of the granules were enhanced. Furthermore, interparticle pore size was reduced from 30 nm to 18 nm by increasing the solid-loading from 25.5 to 51 vol.%.

Umaran et al. prepared composite ceramic slurries (60.73 wt% clay ($d_{50}$: 32.34 $\mu$m),

22.63 wt% feldspar ($d_{50}$: 27.99 $\mu$m) and 16.64 wt% quartz ($d_{50}$: 36.83 $\mu$m)) with 45, 50, 55, 60 and 65 wt% solid loading and optimized amount of 0.8 wt% polyelectrolyte dispersant. It was observed that viscosity was increased by increasing the solid content. This was explained by the fact that when higher solid content is used, the separation distance between particles is decreased and therefore agglomeration is formed which will hinder the movement and flow of the slurry. The slurries up to 50% behaved nearly in Newtonian fluid whereas the higher solid contents behaved as non-Newtonian fluid and shear thinning was observed for them [58].

Not only for spray drying a slurry with high solid content is more favorable, but also in colloidal ceramic processing it is. The aim for having higher solid content, takes its roots from the fact that the green density of the manufactured ceramic is defined by the density of the slurry. Therefore, optimization of high solid content in the slurry at a relatively low viscosity is always mandatory. The problem with high solid-loading slurries is their high viscosity which will be overcome by making the slurry deflocculated. High solid-loading slurries with high viscosity might block the atomizer in case of spray drying and also might not allow easy casting in case of slip casting.

### 2.5.2 Feed viscosity

The feed viscosity is an important factor determining the size of the droplets being formed by atomization. The viscosity of slurries might have three behaviors: Newtonian, dilatant (shear thickening) and pseudoplastic (shear thinning). As it is shown in Figure 2.14, in the Newtonian behavior, the feed viscosity is constant when shear rate is increased, whereas for the dilatant and pseudoplastic behaviors the viscosity is increased and decreased, respectively. The droplet size is dependent on the viscosity of the slurry at high shear rates of the atomizer, not the viscosity at the shear rate of the rheometer. The problem with a dilatant slurry is that its viscosity might increase at high shear rate of the atomizer which results to the formation of imperfect droplets [38].

When the feed has a high viscosity, viscous forces will reduce the energy provided by the nozzle to break the feed into droplets. This reduction in energy will result in larger droplets. Therefore, less viscous slurries are required in order to achieve smaller droplets. This fact can also be described by Equation 2.8.

$$\frac{D_2}{D_1} = (\frac{\mu_2}{\mu_1})^{-0.2} \tag{2.8}$$

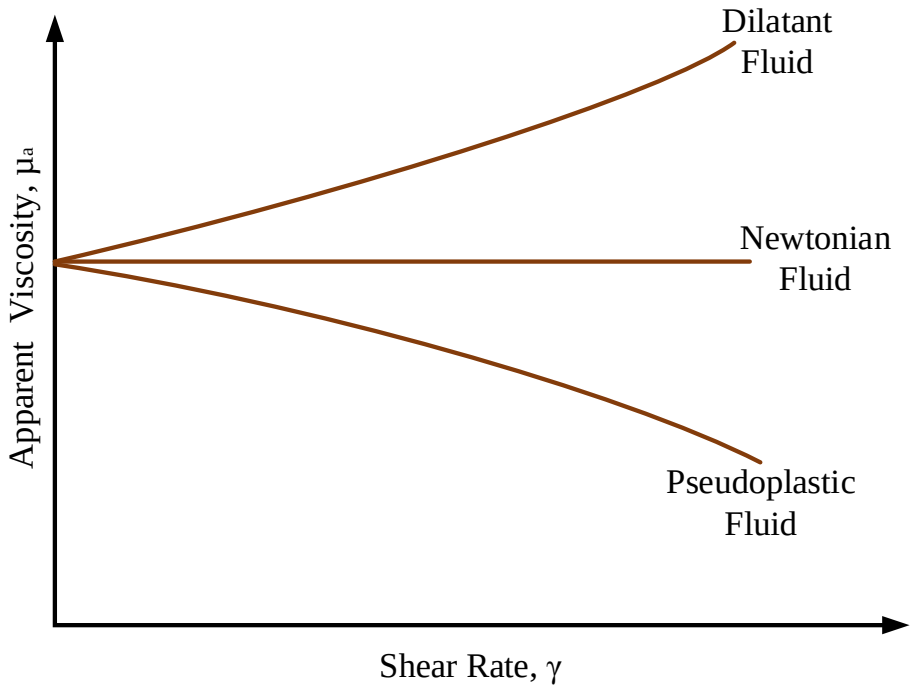


***Figure 2.14*** *Apparent viscosity as a function of shear rate for dilatant, newtonian and pseudoplastic fluids [38].*

where $D_2$ and $D_1$ denote the size of the droplet when the viscosity changes from $\mu_2$ to $\mu_1$ [2].

In a study, two different solid dispersions prepared by acetone/methanol and acetone/water were used for spray drying. The viscosity of the acetone/methanol solution (0.554 cP) was lower than the viscosity (1.39 cP) of acetone/water solvent mixture. They showed that the size of the spray-dried particles made from acetone/-methanol was smaller compared to the size of the particles made from acetone/water. This could be anticipated by the fact that evaporation happens quicker in the less viscous solution [59].

### 2.5.3 Dispersant

The dispersion of powder in the solvent for spray drying or slip casting is very important in such a way that particles should not sediment quickly but they should suspend in the slurry. The micro or nanoparticles present in the slurry are subject to two different forces: van der Waals (attractive) and electrical (repulsive). The properties of powder suspension are mainly due to the interaction of the mentioned forces. The repulsive forces are required to be optimized in order to negate the attractive forces which are responsible for agglomeration formation. By adjusting

the pH of the suspension or by adsorption of charged chemical particles such as dispersants, the charge of a soluble particle in a slurry is changed [38]. The double-layer thickness ($\frac{1}{K}$) which can be defined as "the effective distance which this charge extends into space" is calculated by the Equation 2.9.

$$\frac{1}{K} = \sqrt{\frac{\varepsilon_{\circ}\varepsilon_{r}RT}{4\pi F^{2}\Sigma c_{i}Z_{i}^{2}}} \tag{2.9}$$

where $\varepsilon_{\circ}$, $\varepsilon_{1}$, $R$, $T$, $F$, $c_i$ and $Z_i$ are the permittivity of the air, the dielectric constant of the dispersion medium, the gas constant, the absolute temperature, the Faraday constant, the concentration and the charge of counterions in the dispersion medium, respectively.

As Equation 2.9 shows, the double-layer thickness is inversely proportional to the square root of the concentration of the added ions with opposite charge compared to the charge of the particles in the suspension. Therefore, when the concentration of the ions being released in the suspension is increased, the double-layer thickness will be compressed or decreased. As a result, the energy barrier will be decreased leading to particle agglomeration or flocculation in the slurry [38].

Alumina suspension without any additives has its natural pH 8.5 and the particles are found to have slight positive charge. In order to avoid agglomerations and have a well-dispersed suspension, particles should have high surface charge which generates repulsive forces between the particles [60]. Addition of dispersant into suspension or varying the pH of the suspension are the main ways to change the surface charge.

Dispersants are referred as polyelectrolytes which are added to the dispersing medium (usually water) in order to control the surface charge of the suspended powders. Typically, these polyelectrolytes are one form of polymers with an electronic charge being available through the whole polymer chain whereas the other polymers possess a charged species only at the end of the polymer. Polyacrylic acid (PAA), polymethylacrylic acid (PMAA) and also their salts driven from carboxylic acid group are considered as commonly used dispersants [61].

Dispersants or deflocculants can decrease dramatically the viscosity of a slurry with high solid-loading. In order to achieve a stable slurry, it is always advisable to determine which kind of dispersant should be used for a specific ceramic powder as well as the optimized amount of that. Although dispersants will decrease the viscosity, adding higher than the optimized amount will increase the viscosity because of the presence of rigid flocs which are probably formed due to bridging or depletion

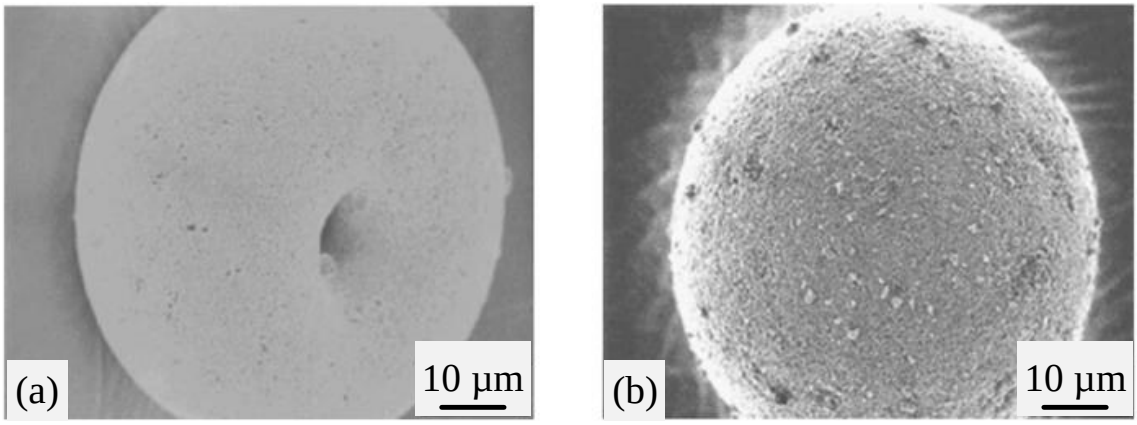


***Figure 2.15*** *External structure of the spray-dried granules from (a) dispersed and (b) flocculated slurries [45].*

flocculation [62].

In a study done by Singh et al., it was shown that the isoelectric point (IEP) of alumina without using any dispersant is 8.5 whereas by using albumin or dibasic ammonium citrate (DAC) it is shifted towards more acidic pH. This shift can be due to the fact that the negatively charged carboxylic group of the dispersant is absorbed on the slightly positively charged surface of alumina and therefore, it will be significantly negatively charged. In this study, it was also proved that the surface charge is not a function of solid-loading; the required amount of dispersant at lower solid contents should hold for the higher solid contents as well [60].

The effect of adding dispersants on the morphology of the spray-dried granules was studied in several experimental works. For example in a study, two alumina ($d_{50}$: 0.46 $\mu$m) slurries were prepared in which the only difference was the amount of the dispersant(Ammonium polyacrylate): 0.4 wt% (dispersed slurry) and 0.2 wt% (flocculated slurry) [45]. The rheological behavior of the suspensions showed that the flocculated slurry had higher viscosity than the dispersed slurry [45]. By spray drying both of the slurries, spherical granules were achieved as it is shown in Figure 2.15. In case of the dispersed slurry, by the flow of water from interior to exterior, the particles are also drawn close to the surface and as drying proceeds an internal hole will be left behind (Figure 2.15 (a)). On the other hand, in case of flocculated slurry which consists of agglomerations, primary particles are in contact with each other because of the van der Waals forces between them. Therefore, water can easily migrate and evaporate without carrying the loosely packed agglomerations along its flow and as a result solid structures are formed (Figure 2.15 (b)). The density and average strength of the granules from the flocculated slurry was higher compared to the dispersed slurry [45].

Similar results were also obtained by another work implemented by Kim et al. When 0.25 wt% dispersant(Ammonium polyacrylate) was used in the composite slurry ($ZrO_2/Al_2O_3$), particles were not carried along to the surface due to the flocculated nature of the slurry and therefore, solid granules were formed. However, when 0.3 wt% was used, the particles were finely dispersed and hollow granules were formed which had lower average and packing density compared to the solid granules. In this work, slurries with less than 0.2 wt% dispersant had high viscosity and therefore could not be spray-dried. The granules which had been sieved smaller than 149 $\mu$m and larger than 44 $\mu$m were collected [46].

### 2.5.4 Binder

Binder is considered as one of the very efficient ingredients of the suspension which is going to be spray-dried. This ingredient has a strong impact on the flowability of the spray-dried granules, their bulk density and also compaction behavior. The most commonly used binders in spray drying process are PVA, polyethylene glycol (PEG) and polyacrylate which are water-soluble polymers. There are several crucial criteria in order to select binder such as its ability to be burnt out completely and cleanly before sintering and more importantly its capacity to make granules with high enough compact density which can deform easily during compaction. In order to have optimal rheological properties, it is always necessary to know the compatibility of the dispersants and binders if they want to be used in a suspension [63].

In a study, it was proved that relatively high amount of binder result in hollow structure of the granules [46]. In this study, 32.7 vol.% composite slurries ($ZrO_2/Al_2O_3$) with 0.5, 1 and 1.5 wt% binder (polyvinylpyrrolidone (PVP)) were prepared. Hollow granules were achieved by using 1.5 wt% and it was explained by the fact that segregation of the excess amount of the binder could make the surface of the droplet tough enough to decrease the permeability of water. Therefore, water is confined inside the droplet and when it is evaporated, collapse of the vapor bubbles will result in donut-shaped structure. In addition to that, when 0.5 wt% was used, hollow structure could be seen again for the granules and it is probably due to the less yield stress of the slurry which is not sufficient enough for solid structure formation [46].

In a study done by Nampi et al., two 35 vol.% alumina ($d_{50}$: 0.5 $\mu$m) slurries with 0.5 wt% dispersant (Ammonium polyacrylate) and with different amount of binder (1.5 and 4 wt% PVA) were prepared. It was found that the relative density was improved by increasing the amount of binder. However, burn-out problems will occur by the use of higher amount of binder which leads to crack formation. Moreover, it was seen that more homogenous structure was obtained by using 1.5 wt% binder whereas more

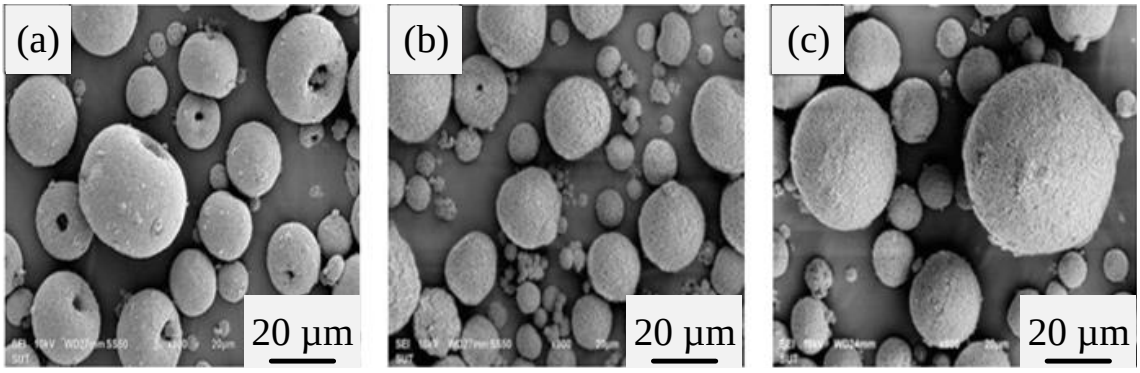


***Figure 2.16*** *Morphology of the spray-dried granules made from (a) PVA, (b) PEG and (c) PVA+PEG binder [54].*

irregularities were observed in the structure of the compact sample due to higher shear strength of the granules made from 4 wt% [63].

In another study, Chiangka used different binders (PVA, PEG, PVA+PEG) in a composite slurry (90 wt% of alumina ($d_{50}$: 1$\mu$m) and 10 wt% of zirconia ($d_{50}$: 0.3$\mu$m)) to examine the effect of binder on morphology and properties of the spray-dried composite granules. The morphology of each granule obtained from different binder is shown in Figure 2.16. It was discovered that large internal voids appeared in the structure of the granules made from the slurry with PVA binder. Although the granules made from the slurry with PEG binder also had internal holes and donut-shaped structure, the hole size was smaller compared to the hole size of the granules made with PVA. Dense spherical structure was obtained for granules with PVA+PEG binder [54].

### 2.5.5 Lubricant

Lubricant is defined as an interfacial phase which reduces the resistance of particles to slide on each other effectively and they are classified into three categories depending on their mechanisms. Lubricants with fluid type are able to supply a low viscous film between sliding particles. In addition to this type, boundary type lubricants can provide very lubricious film which will be absorbed on the surface of the particles. With this type of the lubricants which is mostly used in dry pressing, the surface of the particles will become smoother and also the adhesion between particles is minimized. The third type of lubricants is called solid type which are just fine particles with smooth and laminar surface [14].

Internal lubricants are added to the suspension as an ingredient before spray drying, whereas external lubricants are added to the surface of the granules after spray

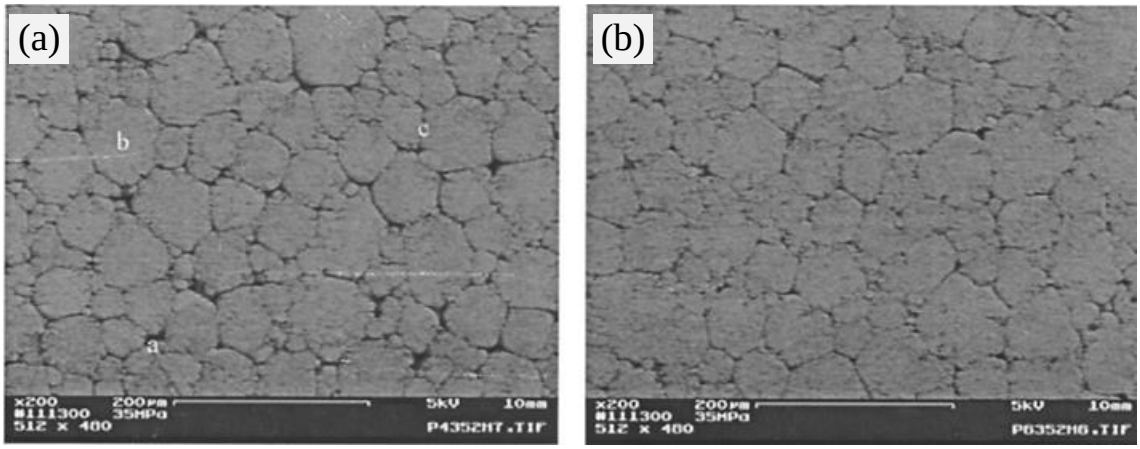


***Figure 2.17*** *SEM image of the compacted structure made from spry dried granules (a) without and (b) with internal lubricant [64].*

drying. The internal lubricants are mixed with primary particles in order to rearrange the particles for reducing the intergranular pores between them. On the other hand, external lubricants are aimed to reduce the friction between the granules and die-wall through compressing the sample and ejecting it from the die [64].

In the study of Nampi et al., after optimizing the amount of binder (PVA) with 1.5 wt% for a 35 vol.% alumina ($d_{50}$: 0.5 $\mu$m) suspension added 0.5 wt% dispersant (Ammonium polyacrylate), two different amounts of internal lubricant (stearic acid), 1 and 4 wt%, were used for spray drying. It was found out that more uniform size distribution was obtained for granules with 4 wt% lubricant. Conversely, less homogenous distribution and more irregular and donut-shaped structures could be observed for the granules with 1 wt% lubricant. Moreover, when granules were compressed and calcined at 1000 °C, less porosity and defects were observed from the granules with 4 wt% lubricant and this can be because of the lower shear strength of the granules which is obtained by the reduction of friction with the presence of lubricant [63].

In another experimental work, two alumina ($d_{50}$: 1.4 $\mu$m) slurries with and without lubricant (ammonium stearate) were spray-dried [64]. The spray-dried powder was sieved and granules with average size of 45-106 $\mu$m were used for this study. It was shown that the size distribution of the granules was not affected by the presence of lubricant. However, the granules with lubricant had higher pressing modulus and also higher green density which indicate better particle packing and pressing efficiency during compaction. It was also demonstrated that the intergranular porosity was reduced from 2.12 % to 1.3 % by the help of lubricant indicating better particle arrangement as it is shown in Figure 2.17.

### 2.5.6 Primary particles

The rheology of a suspension is strongly dependent on the primary particle size and its distribution [65]. Therefore, it is advisable to consider the effect of primary particle size on the morphology and internal structure of the spray-dried granules as well. It is quite well-known that reduction in the primary particle size of the dispersed powder will lead to reduction in the solid-loading of that suspension. This is due to the reason that at a given solid concentration in a suspension, the separating distance between any two particles is decreased by reducing the particle size. Therefore, agglomeration and flocculation may occur in such close encounters [38].

In the study of Ramavath et al., three different alumina powders with different primary particle size of 0.25, 0.8 and 6 $\mu$m were used to prepare alumina suspensions with 30 wt% solid content, 2 wt% binder (PVA) and dispersant (Darvan 821A) for spray drying under identical condition. The morphological structure of the granules made from the primary particle size of 6 $\mu$m consists of agglomerates with distinct voids because of the fast shrinkage of the droplets and surface thickening which prevent the free flow of water vapor. This structure reduced both flowability and apparent density of the granule. On the other hand, granules with fine primary particle size of 0.8 $\mu$m were relatively dense due to the slower shrinkage of the droplets and more uniform distribution of solids. An elastic layer which is formed by organic binders and fine particles lowered the moisture permeability for the granules made from the finest primary particle size 0.25 $\mu$m. Ballooning caused by evaporation was observed in the internal structure of these granules [66].

In another study by Eckhard et al., alumina with 0.5 and 2.5 $\mu$m primary particles were selected to prepare suspensions at comparable solid-loading. The viscosity of the suspension with the finer particles was higher (135.5 mPa.s) than the viscosity of the suspension with coarser particles. This is probably because of the reason that a high number of finer particles in the suspension can provide the system with huge surface area which have to be deluged by the same quantity of water. Thus, less liquid medium is available for the particles to move freely. It was observed that granules from more viscous suspension had denser packed structure with less micro porosities [67].

## 2.6 Compaction

Production of advanced new ceramic composites can be achieved by using spray-dried granules for die pressing [68]. The compaction process requires applying a

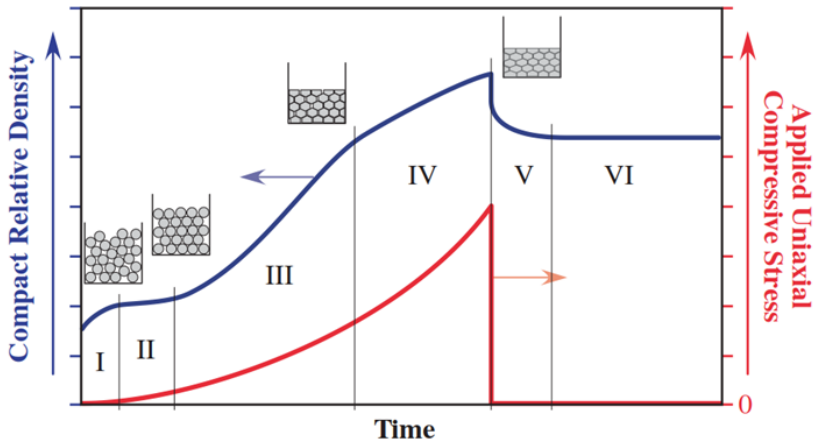


***Figure 2.18*** *Compression behavior of granules [70].*

uniform hydrostatic pressure to the spray-dried granules contained in the die. During this process, large voids between the granules will be reduced by their sliding and rearrangement and after that, the smaller voids will be reduced by deforming and/or fracturing the granules [69]. Dry pressing is involved with the uniaxial compression of spray-dried granules which consist of ceramic primary particles bound together by an organic binder. The schematic compaction plot for this process is depicted in Figure 2.18.

During compression of granules, the relative density of the green body enhances due to the rearrangement and deformation of granules and also the primary particle rearrangement. As it is shown in Figure 2.18, there are different stages involved in compression behavior of granules. During the first stage, the granules are rearranged by applying pressure. Elastic deformation of granules is occurred during the second stage, leading to the extensive plastic deformation and/or fracture of granules during the third stage. During the forth stage, particles are rearranged within the compressed green body. When the compaction pressure is released, the compressed green body expands leading to the relieve of internal stresses. This expansion is occurred as an elastic or instantaneous springback because of the stored energy in the structure. In addition to that, it is occurred as a viscoelastic or time-dependent relaxation because of the viscoelastic properties of the organic binder used for the granulation process. The effect of instantaneous sprinback and time-dependent relaxation is shown during the fifth stage in Figure 2.18. The ultimate density of the compressed green body is obtained during the sixth stage.

The compression behavior of the granules is dependent on several factors such as

granule flowability, applied pressure and friction between the die wall and the granules. Good flowability which is affected by granule morphology and size distribution is a crucial parameter to achieve good compaction. All these factors dictate how granules can fill the die initially and how they rearrange by pressing them. Granules with irregular or dimpled morphology tend to have lower fill and subsequently lower green density compared to the spherical granules [68].

In a study done by Ching-Shan Lin et al., the effect of alumina granule size on the compression behavior of the granules was studied. Five different grades of sieved spray-dried alumina granules and also as-received powders were compressed and their pressed densities were compared. The first powder was larger than 40 mesh, the second powder was ranged between 40 and 80 mesh, the third powder was ranged between 80 and 120 mesh, the fourth powder was ranged between 120 and 180 mesh, the fifth powder was ranged between 180 and 200 mesh and the sixth powder was the as-received alumina powder. It was found that large sieved granules had lower pressed density compared to the smaller sieved granules. Moreover, as-received powders had higher pressed density than the spray-dried granules [69].

In another study done by Somton et al., the effect of alumina granule morphology on the compaction behavior was examined. Four different granules with average size of 41.64, 46.27, 55.27 and 36.71 $\mu$m were studied. The results of their work showed that the granules with hollow structure and a densely packed shell required higher compaction pressures (80 MPa) probably due to the fact that the dense shells needed more force to fracture and fragment them whereas the spherical granules required only 30 MPa. In addition to that, the non-spherical and agglomerated granules had lower packing and tap densities [68].

# 3. RESEARCH METHODS AND MATERIALS

## 3.1 Materials

### 3.1.1 Alumina

In this study, three alumina powders were used for preparing the suspensions. The powders had different nominal work grit size of 0.3, 0.6 and 1 $\mu$m which are labeled by HH300, HH600 and HH1000 in this work, respectively. The properties of the as-received powders are found in Table 3.1 which are provided by the manufacturer.

***Table 3.1*** *Properties of the as-received powders.*

| | $\mathbf{Al_2O_3}$ (%) | $\mathbf{SiO_2}$ (%) | $\mathbf{Fe_2O_3}$ (%) | $\mathbf{Na_2O}$ (%) | $\mathbf{d_{50}}$ ($\mu m$) | **BET** ($m^2/g$) |
|---|---|---|---|---|---|---|
| **HH300** | 99.5 | 0.03 | 0.014 | 0.02 | 0.487 | 7.8 |
| **HH600** | 99.5 | 0.03 | 0.013 | 0.02 | 0.628 | 7.6 |
| **HH1000** | 99.5 | 0.03 | 0.015 | 0.03 | 0.803 | 7.1 |

### 3.1.2 Graphene Oxide

The graphene oxide used in this research work was purchased commercially from Graphenea. The GO sheets were dispersed in water with the concentration of 4 mg/ml. This odorless liquid with the monolayer content of more than 95% had pH of 2.2 - 2.5. The average particle size ($d_{50}$) of the graphene oxide sheets was 14.30 - 16.6 $\mu$m. The elemental analysis of the product can be found in Table 3.2 which is presented by the manufacturer.

### 3.1.3 Dispersant, Binder and Lubricant

The dispersant, binder and lubricant were commercially purchased from Zschimmer & Schwarz. The DOLAPIX CE 64 product (carboxylic acid preparation) was used

***Table 3.2*** *Elemental analysis of the purchased GO.*

| Element | Content Percentage |
|---|---|
| Carbon | 49-56% |
| Hydrogen | 0-1% |
| Nitrogen | 0-1% |
| Sulfur | 2-4% |
| Oxygen | 41-50% |

as dispersant. This organic deflocculating agent had pH of approximately 7 with the density of 1.2 g/cm$^3$. The amount of this product which has to be added to the slurry ranges from 0.1 to 0.5 wt% of the solid content. The OPTAPIX AC 95 product (aqueous polymer dispersion) was used as binder. The pH and density of this product was approximately 9.5 and 1.07 g/cm$^3$, respectively. The amount of this product which has to be added to the slurry ranges from 1.0 to 2.0 wt% of the solid content. The ZUSOPLAST WE 8 product (non-ionic wax dispersion) was used as lubricant. The pH and density of this lubricating agent was approximately 6 and 0.95 g/cm$^3$, respectively.

## 3.2 Research Methods

### 3.2.1 Preparation of the suspensions

In order to prepare the un-doped suspensions, first deionized water was mixed with dispersant, binder and lubricant sequentially. The aqueous medium was stirred for 5 min by the mixer (ULTRA-TURRAX T 50 basic, IKA-WERKE) and then alumina powder was gradually added to the medium. In case of the doped suspensions, first GO was stirred with the deionized water for 5 min and then the subsequent steps were followed same as the steps of preparing the un-doped suspensions. The prepared suspensions were stirred for the period of at least 20h with 6,000 rpm. Formulation of each slurry can be found in Table 3.3. Each slurry is labled by HHX-Y where X represents the size of the alumina primary particle in nm and Y stands for the added amount of GO (vol.%) scaled by $10^{-3}$. As an example, HH300-065 represents the suspension in which 0.065 vol.% GO is incorporated into the alumina matrix with the primary particle size of 300 nm.

***Table** 3.3 Formulation of the prepared suspensions.*

| Suspension | $Al_2O_3$ (wt%) | Dispersant (wt%) | Binder (wt%) | Lubricant (wt%) | GO (vol.%) |
|---|---|---|---|---|---|
| **HH1000-00** | 70/72.5 | 0.3 | 1.5 | 0.3 | - |
| **HH1000-065** | 65/70 | 0.3 | 1.5 | 0.3 | 0.065 |
| **HH1000-195** | 55 | 0.3 | 1.5 | 0.3 | 0.195 |
| **HH600-00** | 70/75/80 | 0.3 | 1.5 | 0.3 | - |
| | 60/65 | 0.2 | 2 | 0.5 | - |
| **HH600-065** | 55 | 0.3/0.4 | 2 | 0.5 | 0.065 |
| **HH600-195** | 45 | 0.3 | 2 | 0.5 | 0.195 |
| **HH300-00** | 50/55 | 0.2 | 2 | 0.5 | - |
| **HH300-065** | 50 | 0.3 | 2 | 0.5 | 0.65 |
| | 55 | 0.4 | 2 | 0.5 | 0.65 |
| **HH300-195** | 40 | 0.3 | 2 | 0.5 | 0.195 |

### 3.2.2 Rheological study

The rheological behavior of each suspension was determined by rheometer (Haake RS 150, RheoStress, Karlsruhe, Germany) performed with a controlled shear rate. In these experiments which were operated at 25 °C, 8.2 ml of each suspension was poured into the cylindrical Z20 DIN geometry. The shear rate was loaded from 0 to 1200 $s^{-1}$ and finally was downloaded from 1200 to 0 $s^{-1}$. In order to avoid the effect of sedimentation in the suspension, measurements were done right after taking the suspension from stirring.

### 3.2.3 Spray drying

Spray drying the prepared suspension was carried out by a industrial size spray dryer (NIRO ATOMIZER, Copenhagen-Denmark) shown in Figure 3.1. After switching on the heating buttons (37.8 kW) and fan of the system, when outlet temperature reached to 110 °C, water was pumped with the local reference of 15,000 rpm in order to heat up the spray dryer. The feeding rate was adjusted in a way to have constant outlet temperature of 107 °C. After 10 min, the valve of the water container was closed and the suspension which was under motion with stirring blade in a different container was pumped into the system with the local reference of 25,000 rpm. The feeding rate was adjusted in a way to have constant outlet temperature of 110 °C. When the suspension got over, the valve of the suspension container was closed and once again the valve of water container was opened to pump water into the system with the local reference of 15,000 rpm. The outlet temperature at this stage should


***Figure 3.1*** *Spray dryer.*

not reach below 100 °C. After a while, the heating buttons were switched off and when the outlet temperature reached to 105 °C, the water valve and the pumping system were closed and turned off. In order to obtain the granules deposited on the wall surfaces, the spray dryer chamber was vibrated. When the outlet temperature reached to 45 °C, fan of the spray dryer was switched off and granules were collected from the separation flask and product vessel. The last step was devoted to clean and wash the spray dryer and the atomizer.


***Figure 3.2*** *Scanning electron microscope (SEM).*

### 3.2.4 SEM characterization of the as-received powders and the spray-dried granules

In order to characterize the morphology of the as-received powders and spray-dried granule, scanning electron microscope (SEM) was used. The powders were poured on the carbon tape which was attached to the SEM sample holder. Pressurized air was used to remove excess of loose and unattached powders on the carbon tape. The powders were coated by gold with the use of S150 SPUTTER COATER. SEM images were taken by the scanning electron microscope (XL30, Philips) shown in Figure 3.2. Secondary electrons with 20 kV accelerating voltage were used for imaging.

### 3.2.5 Compressive strength

The granule compression tests were performed by Instron 5967 (Illinois Tool Work Inc., USA) shown in Figure 3.3. This materials tester uses a load cell with the maximum load capacity of 30 kN and accuracy of $\pm 0.1\%$. Compaction of granules was performed in a cylindrical die with linear plate heads. This tool consists of a cylindrical die with diameter of 19.5 mm in which the granules were poured, a top punch and a bottom punch. First, all the surfaces which were in contact with

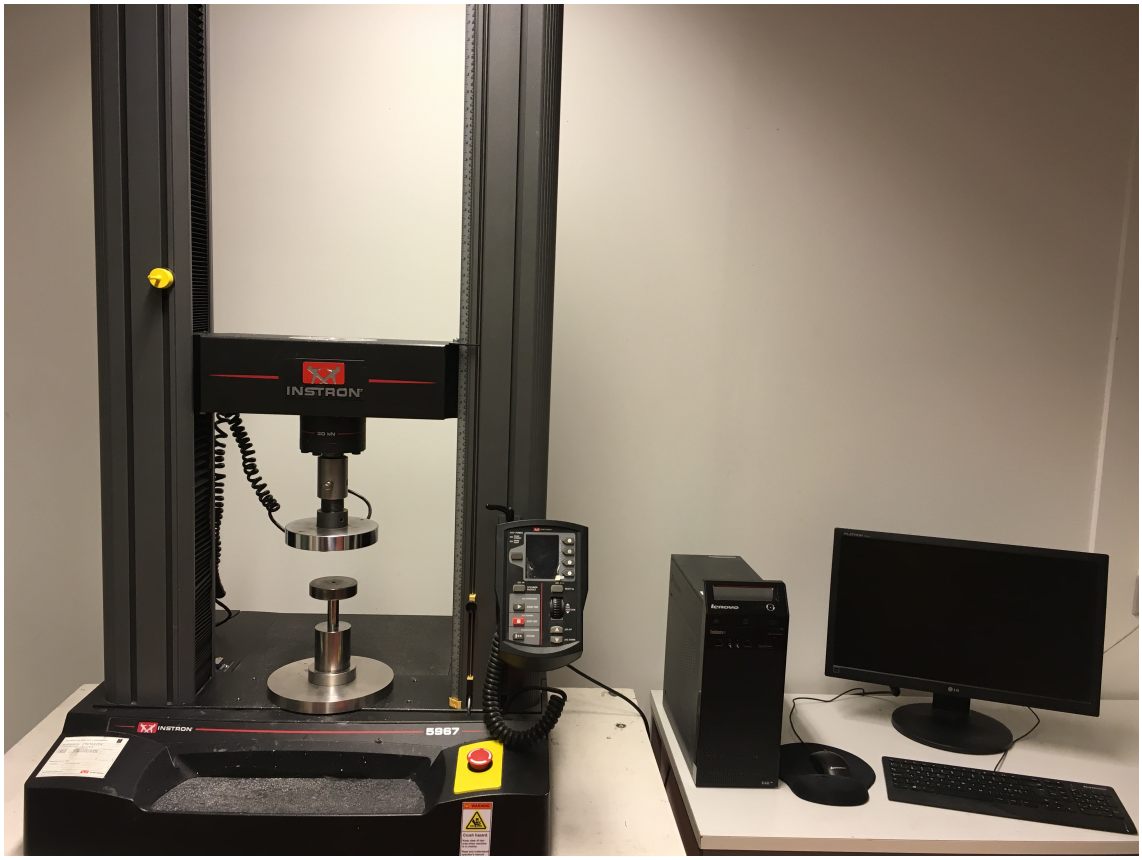


***Figure 3.3*** *Instron 5967.*

the granules were sprayed with silicon (saBesto, Würth) and then slightly wiped with tissue in order to control wall friction. 4 g of each sprayed dried granules was measured and determined by a precision scale (Mettler AE163, GWB, Switzerland) with accuracy of 0.01 mg. The granules were poured into the die which was located on top of the lower punch. Then the tool was tapped in order to make the surface of the granule bed smooth and leveled. Subsequent to that, the top punch was smoothly put into the cylindrical die and it was pressed by a flat steel attached to the load cell while the lower punch was unmoved during the compression test. The samples were compacted by 33.5 MPa at a constant speed of 1.00 mm/min.

# 4. RESULT AND DISCUSSION

## 4.1 Characterization of the as-received powders

### 4.1.1 EDS analysis

All the as-received powders where subject to energy-dispersive x-ray spectroscopy (EDS) analysis in order to check the purity of them. The chemical composition of the powders is shown in Figure 4.1. The EDS data shows a major peak of Al and smaller peaks of Au, C and O elements. The peaks associated to Au and C can be justified by the fact that the powders were poured on the carbon tape and coated by gold for the SEM characterization. According to the data, by excluding the Au, C and O elements, all the three powders were composed of 100% Al with no major impurities.

### 4.1.2 SEM characterization

The SEM images of the as-received powders is shown in Figure 4.2. As it can be seen, particles have different irregular geometric shapes with different aspect ratios and are mainly agglomerated and stacked on each other. A rough estimation of the particle size of the as-received powders is in accordance with the data provided by the manufacturer.

## 4.2 Formulation of the colloidal suspensions

Formulation of the slurries with the aim of achieving spherical spray-dried granules with the highest solid content was based on the rheological characterization and SEM characterization of the spray-dried granules in parallel. In the following sections, the viscosity of un-doped and doped suspensions and morphology of the spray-dried granules obtained from them will be discussed in detail.

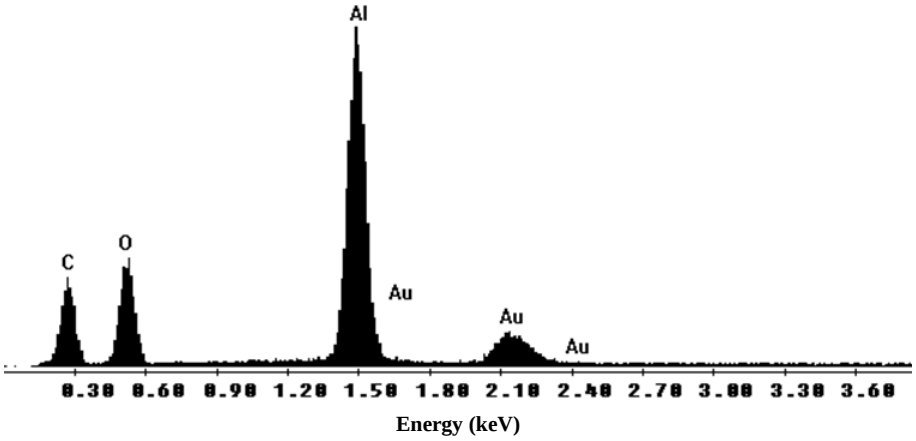


***Figure 4.1*** *Chemical composition of the as-received powders.*

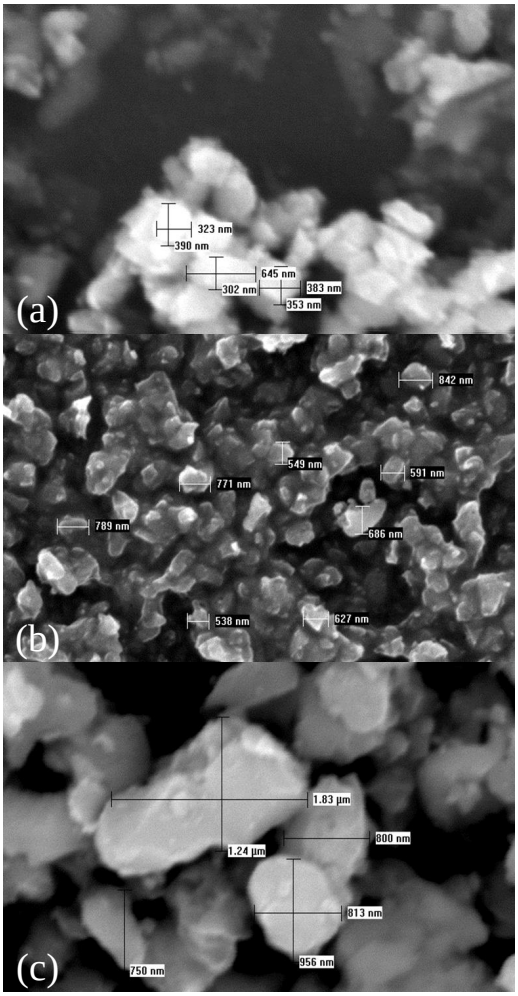


***Figure 4.2*** *SEM images of the as-received powders with the primary particle size of (a) 0.3 µm, (b) 0.6 µm and (d) 1 µm.*

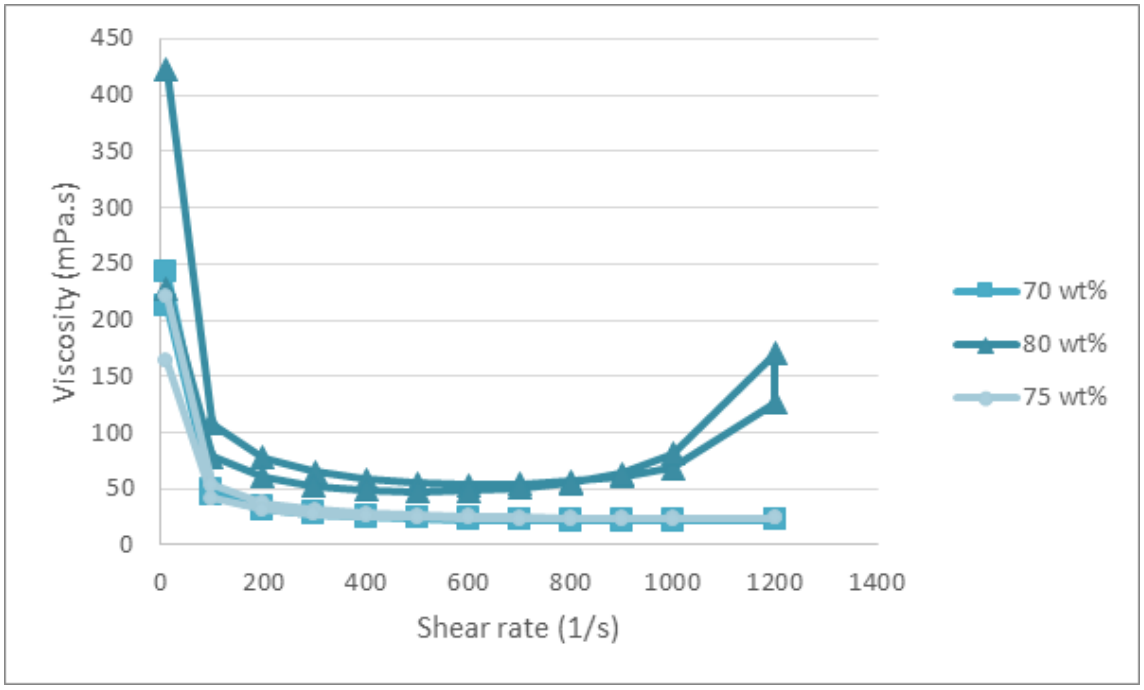


***Figure 4.3*** *Viscosity vs. shear rate for 70, 75 and 80 wt% solid-loading alumina (0.6 μm) suspensions.*

### 4.2.1 Un-doped suspensions

#### HH600-00

Preparation of the un-doped suspensions was initiated by the as-received alumina powder with the primary particle size of 0.6 $\mu$m. As the first batch, 0.3 wt% of dispersant, 1.5 wt% of binder and 0.3 wt% of lubricant were selected to be added in the suspension. A series of suspensions with varying solid loading (70, 75 and 80 wt%) were prepared and the rheological behavior of them were measured. Figure 4.3 shows the viscosity of these suspensions as a function of shear rate.

As it can be seen from Figure 4.3, although viscosity at low shear rates (10 $s^{-1}$) is high, 242, 221 and 423 mPa.s for the 70, 75 and 80 wt% suspensions relatively, it reduces as the shear rate increases. This illustrates the shear thinning behavior in which by shearing the suspension, the present flocs break down and consequently it causes the resistance to flow reduces. Moreover, during the low shear rates, reduction of the viscosity for each curve is fast. However, when shear rate reaches to a certain value, the viscosity curves become smooth. The rheological behavior of the 70 and 75 wt% suspensions were alike with the viscosity of 22 and 23 mPa.s at the shear rate of 1200 $s^{-1}$.

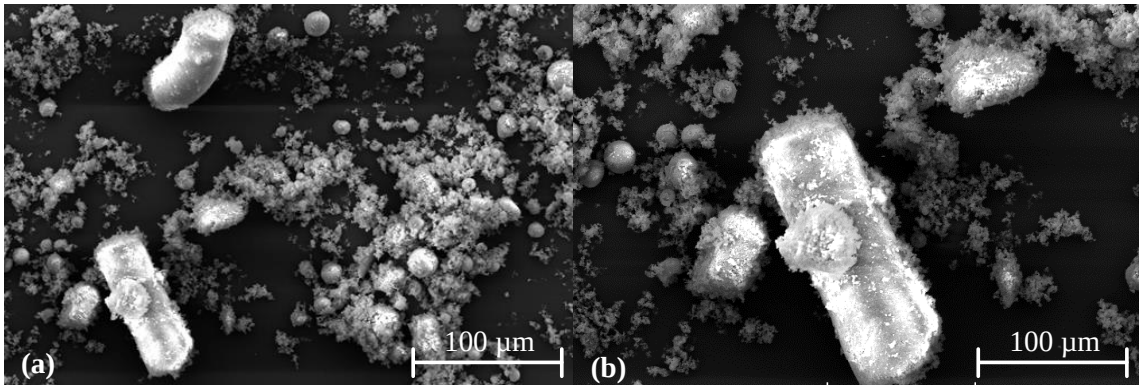


***Figure 4.4*** *Morphology of the spray-dried granules from the suspension with 80 wt% alumina (0.6 µm), 0.3 wt% dispersant, 1.5 wt% binder and 0.3 wt% lubricant.*

The higher viscosity of the suspension with 80 wt% content compared to the viscosity of the other suspensions is due to the presence of more flocs in this suspension as the particle number and their associated interactions are higher. The shear thinning behavior is observed for this suspension up to 900 $s^{-1}$ at which the viscosity is 60 mPa.s. However, after this shear rate (900 $s^{-1}$), shear thickening behavior in which the viscosity increases by increasing the shear rate can be observed for this suspension. The viscosity was increased steadily and it reached to 169 mPa.s at the shear rate of 1200 $s^{-1}$. This behavior can be explained by the regeneration of flocs in a highly concentrated suspension after a certain shear rate which leads to the increase of viscosity. Dilatant suspensions are undesirable for spray drying since at high shear rates of the atomizer, the suspensions become very stiff to flow smoothly. This matches with the SEM images of the suspension with 80 wt% solid content, shown in Figure 4.4, which depicts huge irregular and rod shaped spray-dried granules.

The morphology of the spray dried granules from the 70 wt% suspension is shown Figure 4.5 (a, b). As it is shown, the granules have donut-shaped structure (Figure 4.5 (a)) and also some irregular and rod-shaped structures can be detected (Figure 4.5 (b)). As it can be observed from Figure 4.5 (c, d), the presence of the huge irregular structures was more pronounced in the spray-dried granules obtained by the 75 wt% suspension. In other words, the size distribution of the granules obtained from 70 wt% suspension was more homogenous and narrow compared to the granules obtained from 75 wt%. This can be explained that the energy provided by the nozzle in order to break the droplets was reduced by the presence of the viscous forces which are due to the interactions of the higher particle number present in 75 wt% suspension. As a result of this reduction in energy, larger granules will be formed. Therefore, it was concluded that it is not possible to obtain spherical granules with

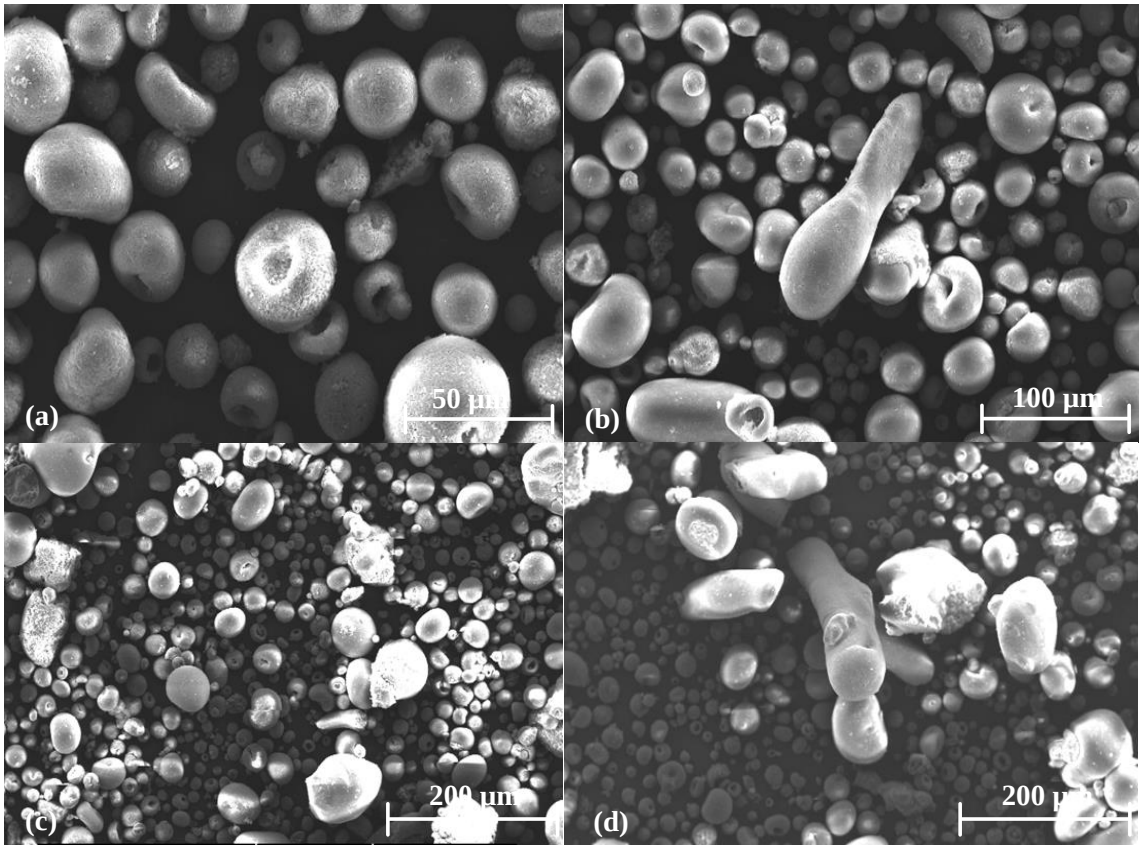


***Figure 4.5*** *Morphology of the spray-dried granules from the suspension with 0.3 wt% dispersant, 1.5 wt% binder, 0.3 wt% lubricant and (a, b) 70 wt% alumina (0.6 µm) and (c, d) 75 wt% alumina (0.6 µm).*

75 wt% solid content and the solid-loading should be decreased.

The presence of the donut-shaped and hollow granules implies the fact that by using 0.3 wt% dispersant, the suspension was dispersed well. The suspensions were stabilized by the electrosteric repulsion. During this stabilization, the adsorbed anionic polyelectrolyte provided a steric barrier of interaction between the alumina particles. This significant repulsion between the particles hindered them to form any agglomerations or flocs. In this case, with the flow of water from the interior to exterior, the suspended particles were also carried along towards the surface and left a void behind, as it is evident in the Figure 4.5.

However, in order to achieve solid spherical granules, the suspension has to be slightly flocculated and therefore, it was decided to reduce the amount of dispersant to 0.2 wt%. By reducing the amount of dispersant, due to the mutual attraction between the particles, floc groups or networks were formed. In addition to that, the obtained granules could not be compressed well with 100 MPa and the compressed structures were broken easily while ejecting from the die. Therefore, the second

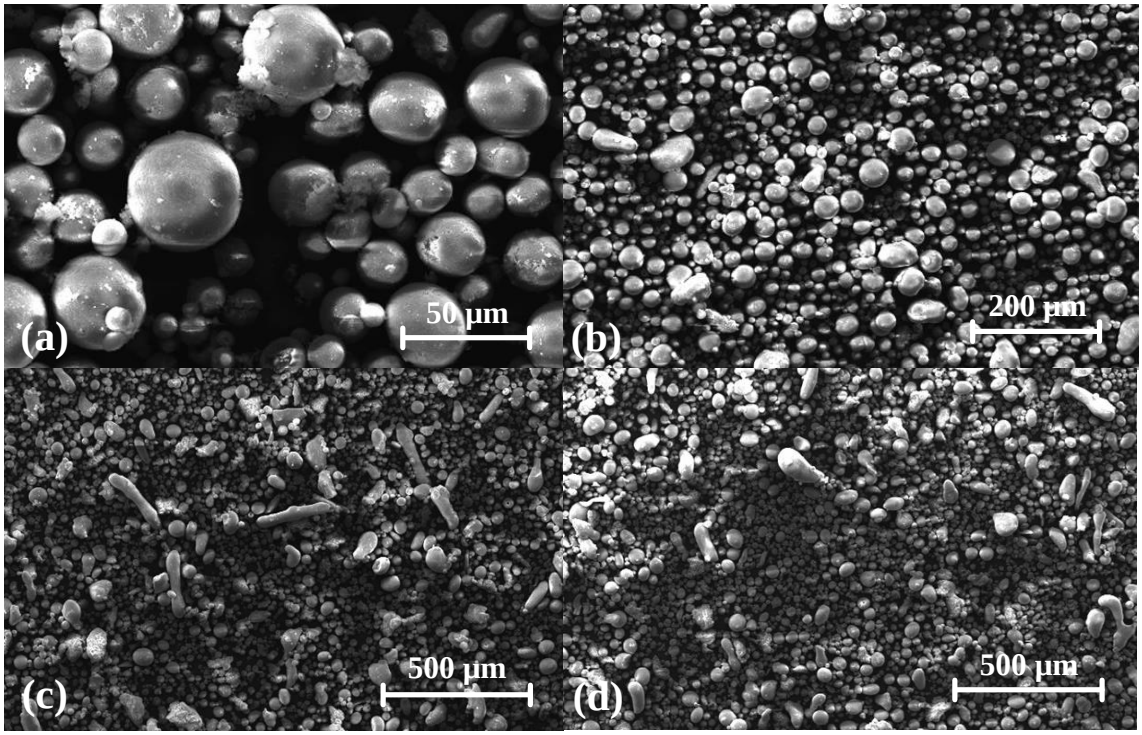


***Figure 4.6*** *Morphology of the spray-dried granules from the suspension with 0.2 wt% dispersant, 2 wt% binder, 0.5 wt% lubricant and (a, b) 60 wt% alumina (0.6 µm) and (c, d) 65 wt% alumina (0.6 µm).*

batch for the formulation of the suspension with this as-received powder was based on choosing 0.2 wt% dispersant, 2 wt% binder, 0.5 wt% lubricant and with the varying solid contents (65 and 70 wt%). The morphology of the spray-dried granules obtained from the 65 and 70 wt% suspensions are shown in Figure 4.6 (a, b) and (c, d), respectively.

As it can be seen from Figure 4.6 (a, b), the granules have solid spherical structures. This proves that the suspension was slightly flocculated. In this case, the primary particles are attracted to each other through the van der Waals forces, creating agglomerations. Therefore, water can easily migrate through these agglomerations without carrying them towards the external surface. Eventually after the evaporation of water, solid structures are formed. On the other hand, even though granules obtained from the suspension with 70 wt% solid content do not have donut-shaped structure, more rod shaped structures can be observed for them. This indicates that this solid content is too high for spray drying a suspension with the aforementioned formulation and primary particle size. The optimized formulation for the HH600-00 suspension is found in Table 4.1.

***Table 4.1*** *Formulation of the HH600-00 suspension.*

| Suspension | $Al_2O_3$ (wt%) | Dispersant (wt%) | Binder (wt%) | Lubricant (wt%) | GO (vol.%) |
|---|---|---|---|---|---|
| **HH600-00** | 60 | 0.2 | 2 | 0.5 | - |

### HH1000-00

Formulation of the HH1000-00 suspension can be achieved according to the finalized formulation of the HH600-00 suspension obtained in the previous section. In this case, the average primary particle size, 1 $\mu$m, is larger than 0.6 $\mu$m and therefore particles have less surface area and more particles can interact with each other. The separating distance between two particles with 1 $\mu$m is larger than the separating distance between two particles with 0.6 $\mu$m. Hence, more solid content ($>$ 65 wt%) can be suspended in the HH1000-00 suspension without forming agglomerations. The first batch for the formulation of HH1000-00 suspension was based on choosing 0.3 wt% dispersant, 1.5 wt% binder and 0.3 wt% lubricant with the varying solid content of 70 and 72.5 wt%.

The morphology of the spray dried granules from these suspensions is shown in Figure 4.7. As it can be seen from Figure 4.7 (a, b), most of the granules have solid spherical structures and only few donut-shaped structures are available. Moreover, the morphology of some of the granules exhibit craters or so-called blow holes which are formed by an inward collapse of the produced shell during the drying stage. This collapse can occur by the formation of a partial vacuum by the capillary-induced movement of the particles from the inner core region of the droplet to the surface shell. On the other hand, Figure 4.7 (c,d) represents the granules obtained from 72.5 wt% solid content. It is evident that due to the presence of the huge irregular structure, this solid content was too high to achieve spherical granules. The finalized formulation of the HH1000-00 suspension can be found in Table 4.2.

***Table 4.2*** *Formulation of the HH1000-00 suspension.*

| Suspension | $Al_2O_3$ (wt%) | Dispersant (wt%) | Binder (wt%) | Lubricant (wt%) | GO (vol.%) |
|---|---|---|---|---|---|
| **HH1000-00** | 70 | 0.3 | 1.5 | 0.3 | - |

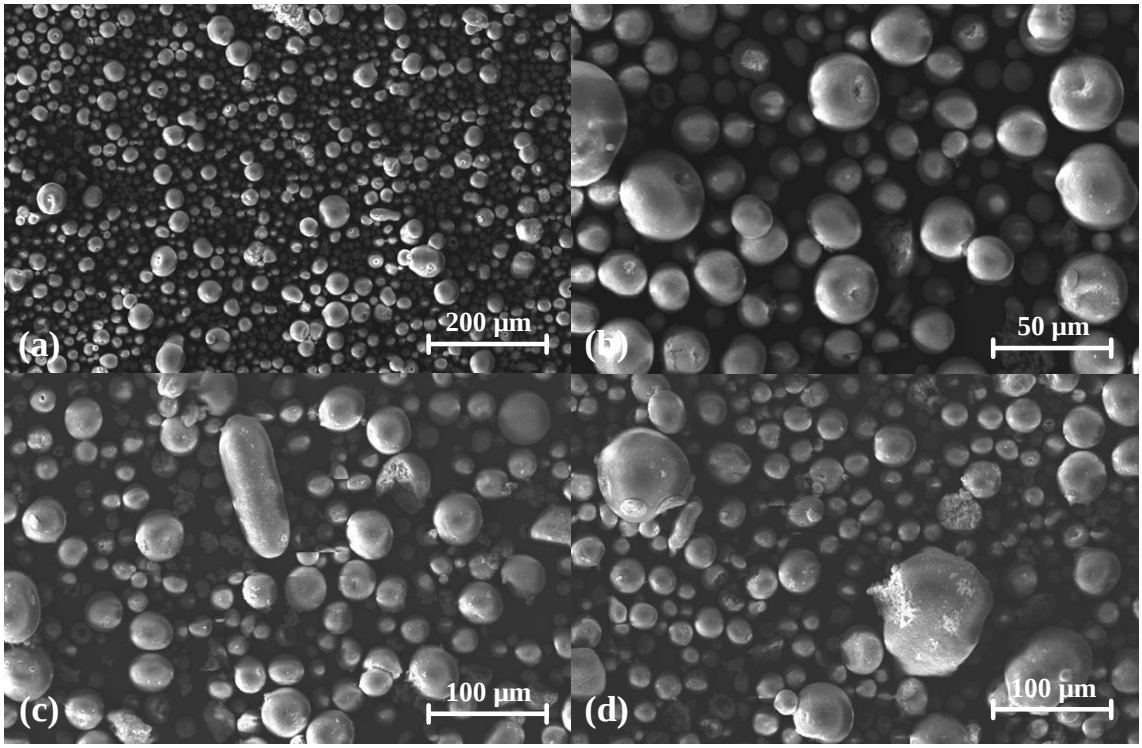


***Figure 4.7*** *Morphology of the spray-dried granules from the suspension with 0.3 wt% dispersant, 1.5 wt% binder, 0.3 wt% lubricant and (a, b) 70 wt% alumina (1 µm) and (c, d) 72.5 wt% alumina (1 µm).*

**HH300-00**

Formulation of the HH300-00 suspension was based on the finalized formulation of the HH600-00 suspension. In this case, as the primary particle size is reduced, higher number of the particles is introduced to the system for a given solid concentration and this creates shorter interparticle distance between individual particles. Therefore, particles in close proximity can easily form agglomerations when a small disturbance in the system such as Brownian motion is happened. In order to avoid the formation of agglomerations in the HH300-00 suspension, it was decided to reduce the solid content aimed for the HH600-00 suspension (65 wt%) to 55 and 50 wt% and utilize 0.2 wt% dispersant, 2 wt% binder and 0.5 wt% lubricant.

The morphology of the spray dried granules obtained from these suspensions is shown in Figure 4.8. As it is depicted in Figure 4.8 (a, b), the granules obtained from the 50 wt% solid content have solid spherical structures with homogeneous size distribution. The surface of these granules is more even and smoother compared to the granules obtained from the HH600-00 and HH1000-00 suspensions which is probably due to the fine submicron primary particles of the HH300-00 suspension.

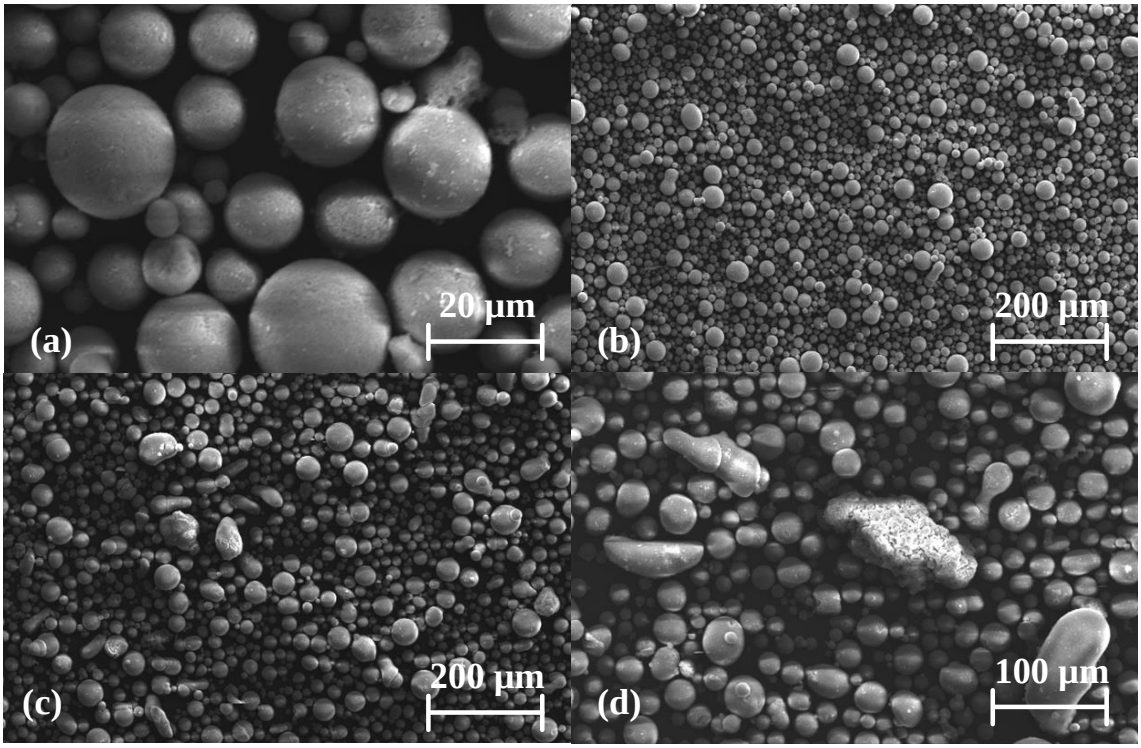


***Figure 4.8*** *Morphology of the spray-dried granules from the suspension with 0.2 wt% dispersant, 2 wt% binder, 0.5 wt% lubricant and (a, b) 50 wt% alumina (0.3 µm) and (c, d) 55 wt% alumina (0.3 µm).*

On the other hand, irregular and rod shaped structures are more seen among the granules obtained from the suspension with 55 wt% solid content (Figure 4.8 (c, d)) which indicates that this solid content was too high. Therefore, the finalized formulation of the HH300-00 can be found in Table 4.3.

***Table 4.3*** *Formulation of the HH300-00 suspension.*

| **Suspension** | **$Al_2O_3$ (wt%)** | **Dispersant (wt%)** | **Binder (wt%)** | **Lubricant (wt%)** | **GO (vol.%)** |
|---|---|---|---|---|---|
| **HH300-00** | 50 | 0.2 | 2 | 0.5 | - |

### 4.2.2 Doped suspensions

The main challenge in this study was to formulate the alumina suspensions doped with GO for spray drying since it increased the viscosity of the prepared suspensions significantly which will be discussed in detail in the following sections. However, it is worthwhile to discuss the reasons of this significant enhancement of the viscosity in general prior to going through the formulation trials for each doped suspension.

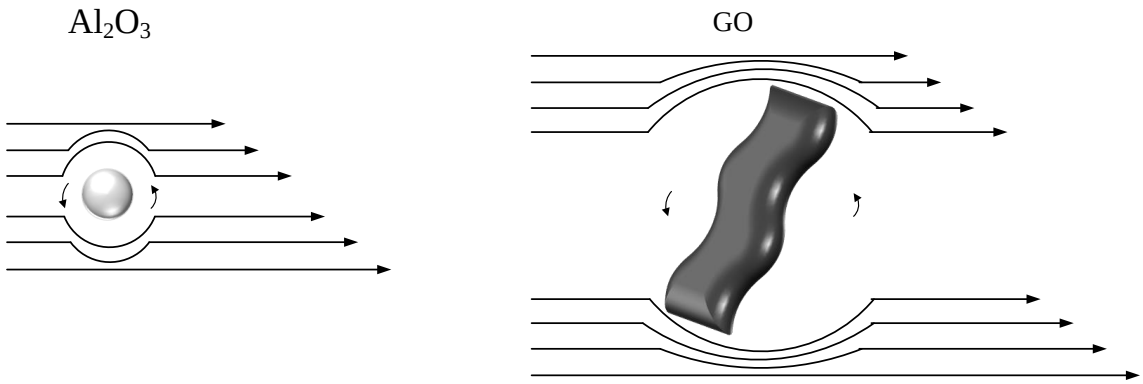


***Figure 4.9*** *Schematic diagram of the hydrodynamic volume of $Al_2O_3$ and GO.*

Firstly, all the particles suspended in the slurry will be rotated under an applied shear stress. Therefore, when the suspension is introduced to the presence of nonspherical particles, the maximum solid content has to be decreased due to the larger effective hydrodynamic volume of the nonspherical particles. The hydrodynamic volume of a particle is the volume which is swept out by that particle as it rotates in the suspension. It is assumed that particles move in the suspension as the equivalent impermeable particles with their correspondent hydrodynamic volume [71].

In case of the alumina suspensions doped with GO, the hydrodynamic volume of the suspended particles is shown in Figure 4.9. This schematic diagram is based on assuming the micron and submicron alumina particles to have spherical structures. As it can be observed, the GO sheets used in this study with the average lateral dimension of 16 $\mu$m have larger hydrodynamic volumes compared to the hydrodynamic volume of the small alumina particles (0.3, 0.6, 1 $\mu$m). When the suspension is introduced to a shear stress, the lamina layers move with different velocities. The particle is spanned to the direction of the layer with the highest velocity. This tendency to spin the particles requires the least energy when the particle is spherical. Therefore, the viscosity of the suspension is increased by the presence of GO due to the difference in energy which is required to force the solvent around and past the suspended particles. As the result of this increase in viscosity, the solid content has to be decreased when GO is added to the suspension.

Secondly, the GO sheets possess polar oxygen-containing functional groups such as carbonyl, hydroxyl and epoxides groups which are located on their basal faces and edges. In addition to these groups, it is believed that carboxylic acid groups are also available at the edge of the GO sheet. The purchased GO for this study was very acidic with the pH 2.5-2.7. This strong acidity of GO proves the presence of a relatively strong acidic group such as -COOH. The presence of this group provides

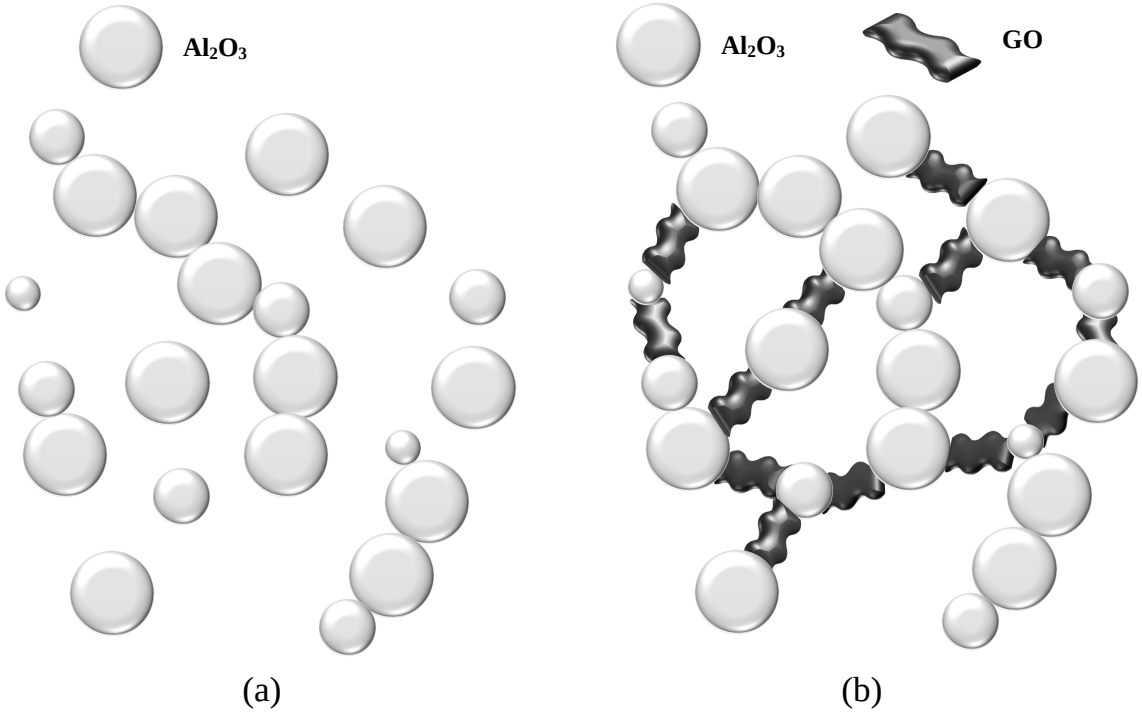


***Figure 4.10*** *(a) Well-dispersed alumina suspension without presence of GO, (b) Flocculated alumina suspension with the presence of GO due to the bridging effect (adapted and modified from [72]).*

the GO sheet with a high negative charge density. Therefore, incorporation of GO into the alumina matrix was achieved by the electrostatic attraction between the negatively charged GO sheets and slightly positively charged alumina powders. As a result of this electrostatic attraction, the GO sheet with its high aspect ratio is able to wrap up partial surface of the suspended alumina particles. At the wrapping interface, GO is considered as a connecting bridge which links two adjacent alumina particles [72]. This bridging effect is shown in Figure 4.10. As a consequence of this effect, the distance between two alumina particles is reduced and they are eventually linked with each other without any direct collisions. Therefore, a continuous chain or network is formed which aggravates the agglomeration of the alumina particles. The presence of these agglomerations in the suspension leads to the increase of the local viscosity and therefore, solid content must be reduced for the alumina suspensions doped with GO.

The increase of viscosity was more significant when the alumina primary particle size was reduced. This is due to the fact that multiple submicron-sized (0.3 and 0.6 $\mu$m) alumina particles can be adsorbed on the large micron sized GO sheets and accordingly, more particles are in contact which increases the viscosity of the suspensions. However, when alumina particles have micron size (1 $\mu$m), less particles

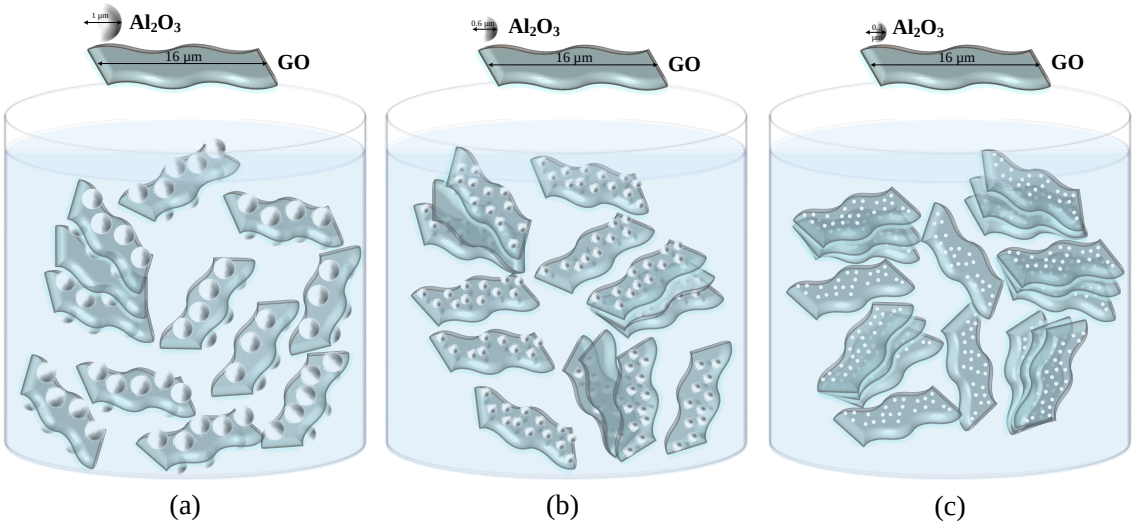


***Figure 4.11*** *Effect of the alumina primary particle size (a) 1 µm, (b) 0.6 µm and (c) 0.3 µm on bridging effect caused by the presence of GO.*

are adsorbed on the GO sheets and the bridging effect is not very significant in this case. The effect of the primary particle size on the bridging effect is shown in Figure 4.11. In the following sections, various formulations for spray drying doped suspensions will be discussed in detail.

### HH1000-065 and HH1000-195

Formulation of the HH1000-065 was based on the finalized formulation of the HH1000-00 suspension. For the first batch, two suspensions with 0.3 wt% dispersant, 1.5 wt% binder, 0.3 wt% lubricant and with various solid content of 70 and 65 wt% were prepared. The viscosity of these suspensions is shown in Figure 4.12. As it can be seen from the curves, addition of GO to the alumina suspensions increased the viscosity. Therefore, only suspensions with 70 and 65 wt% solid content were spray dried. The morphology of the spray dried granules is shown in Figure 4.13. As it can be seen from Figure 4.13 (a, b), irregular and elongated structures can also be found commonly among the spherical granules which excluded this formulation for HH1000-065 suspension to achieve spherical granules. On the other hand, as shown in Figure 4.13 (c, d), granules obtained from 65 wt% suspension had solid spherical structures, indicating that the GO doped alumina suspension with the aforementioned formulation was slightly flocculated. The finalized formulation of the HH1000-065 suspension is found in Table 4.4.

By increasing the amount of the added GO to the suspension from 0.065 to 0.195

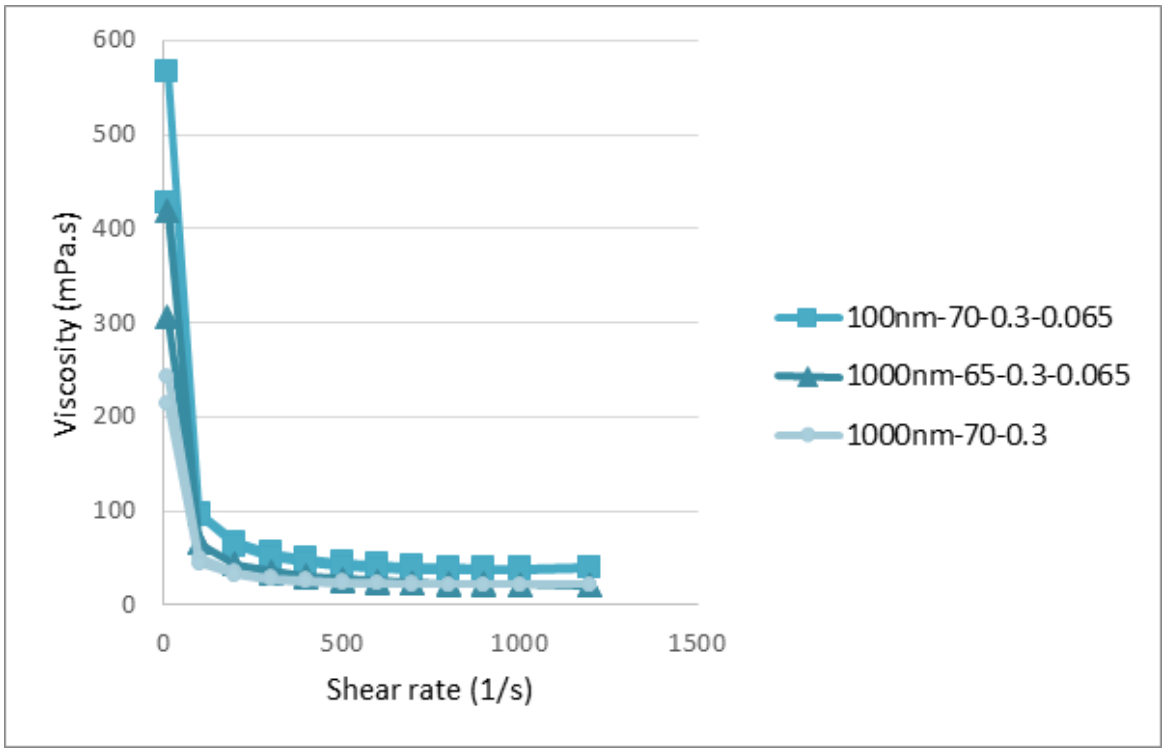


***Figure 4.12*** *Viscosity of un-doped suspensions with 70 wt% almina, 0.3 wt% dispersant, 1.5 wt%binder, 0.3 lubricant and doped suspensions with 0.3 wt% dispersant, 1.5 wt% binder, 0.3 wt% lubricant, 0.065 vol.% GO and varying solid content of 65 and 70 wt% alumina (1 μm).*

***Table 4.4*** *Formulation of the HH1000-065 suspension.*

| Suspension | $Al_2O_3$ (wt%) | Dispersant (wt%) | Binder (wt%) | Lubricant (wt%) | GO (vol.%) |
|---|---|---|---|---|---|
| **HH1000-065** | 65 | 0.3 | 1.5 | 0.3 | 0.065 |

vol.%, viscosity of the suspension was increased and therefore, it was decided to reduce the solid content of the HH1000-065 suspension from 65 wt% to 55 wt% for the HH1000-195 suspension whereas the other additives were not changed. The morphology of the granules obtained by spray drying this suspension, shown in Figure 4.14, was mainly solid spherical without any central voids. The finalized formulation of the HH1000-195 suspension can be found in Table 4.5.

***Table 4.5*** *Formulation of the HH1000-195 suspension.*

| Suspension | $Al_2O_3$ (wt%) | Dispersant (wt%) | Binder (wt%) | Lubricant (wt%) | GO (vol.%) |
|---|---|---|---|---|---|
| **HH1000-195** | 55 | 0.3 | 1.5 | 0.3 | 0.195 |

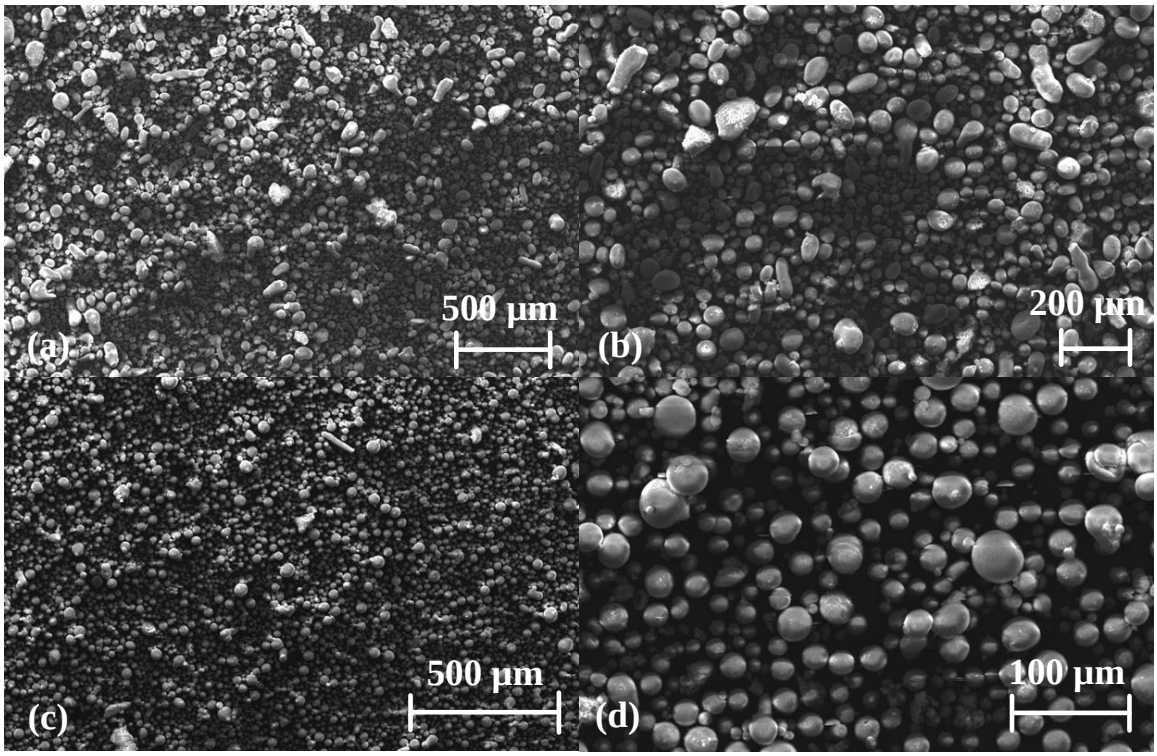


***Figure 4.13*** *Morphology of the spray-dried granules from the suspension with 0.3 wt% dispersant, 1.5 wt% binder, 0.3 wt% lubricant, 0.065 vol.% GO and (a, b) 70 wt% alumina (1 µm) and (c, d) 65 wt% alumina (1 µm).*

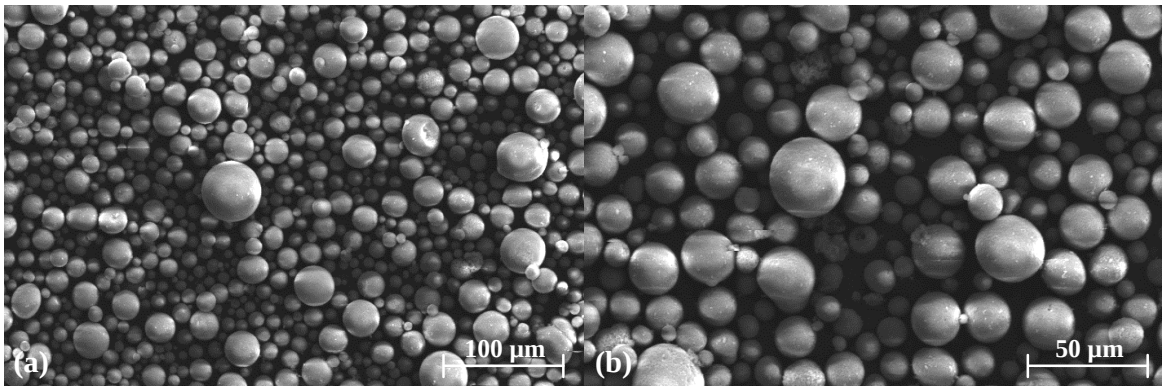


***Figure 4.14*** *Morphology of the spray-dried granules from the suspension with 0.3 wt% dispersant, 1.5 wt% binder, 0.3 wt% lubricant, 0.195 vol.% GO and 55 wt% alumina (1 µm).*

### HH600-065 and HH600-195

The first trial for formulizing the HH600-065 suspension was based on reducing the solid content of the HH600-00 suspension. However, the slurries were too thick and it was not possible to spray dry them. Therefore, it was decided to increase the

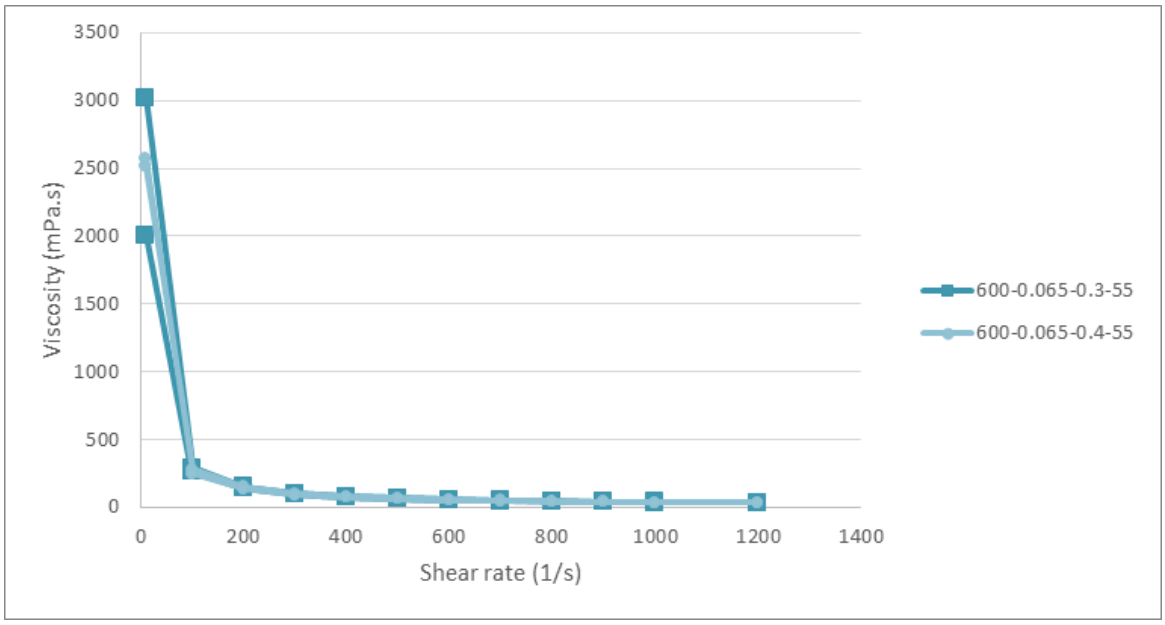


***Figure 4.15*** *Viscosity of suspensions with 55 wt% alumina (0.6 μm), 0.065 vol.% GO, 2 wt% binder, 0.5 wt% lubricant and varying amount of dispersant of 0.3 and 0.4 wt%.*

amount of dispersant from 0.2 to 0.3 and 0.4 wt% with 55 wt% solid content. The rheological behavior of the prepared suspensions was similar, with the viscosity of $\sim$ 33 mPa.s, as it is shown in Figure 4.15.

However, the morphology of the spray-dried granules obtained from these suspensions was different as it is shown in Figure 4.16. The granules obtained from the suspension with 0.4 wt% dispersant had donut-shaped morphology and majority of the granules had blow holes in their structures (Figure 4.16 (a, b)) which will reduce the flowability of the granules. On the other hand, granules obtained from the 0.3 wt% dispersant, had solid spherical structures as shown in Figure 4.16 (c, d). The finalized formulation of the HH600-065 suspension can be found in Table 4.6.

***Table 4.6*** *Formulation of the HH600-065 suspension.*

| **Suspension** | **$Al_2O_3$ (wt%)** | **Dispersant (wt%)** | **Binder (wt%)** | **Lubricant (wt%)** | **GO (vol.%)** |
|---|---|---|---|---|---|
| **HH600-065** | 55 | 0.3 | 2 | 0.5 | 0.065 |

In order to formulate the HH600-195 suspension, solid content was reduced to 45 wt%. Although the hose connecting the suspension container to the atomizer was blocked several times and feed rate had to be increased, solid spherical granules were obtained by spray drying this suspension as shown in Figure 4.17. Formulation of the HH600-195 suspension can be found Table 4.7.

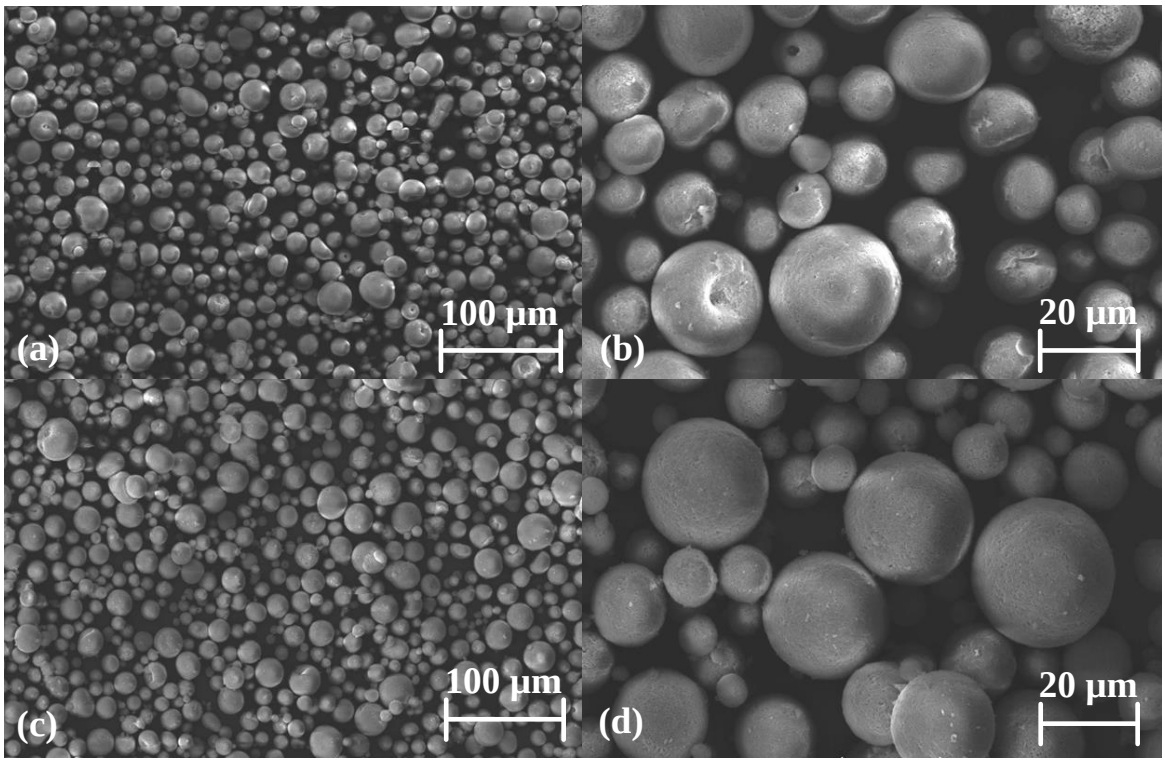


***Figure 4.16*** *Morphology of the spray-dried granules from the suspension with 55 wt% alumina (0.6 µm), 2 wt% binder, 0.5 wt% lubricant, 0.065 vol.% GO and (a, b) 0.4 wt% dispersant, (c, d) 0.3 wt% dispersant.*

***Table 4.7*** *Formulation of the HH600-195 suspension.*

| Suspension | $Al_2O_3$ (wt%) | Dispersant (wt%) | Binder (wt%) | Lubricant (wt%) | GO (vol.%) |
|---|---|---|---|---|---|
| **HH600-195** | 45 | 0.3 | 2 | 0.5 | 0.195 |

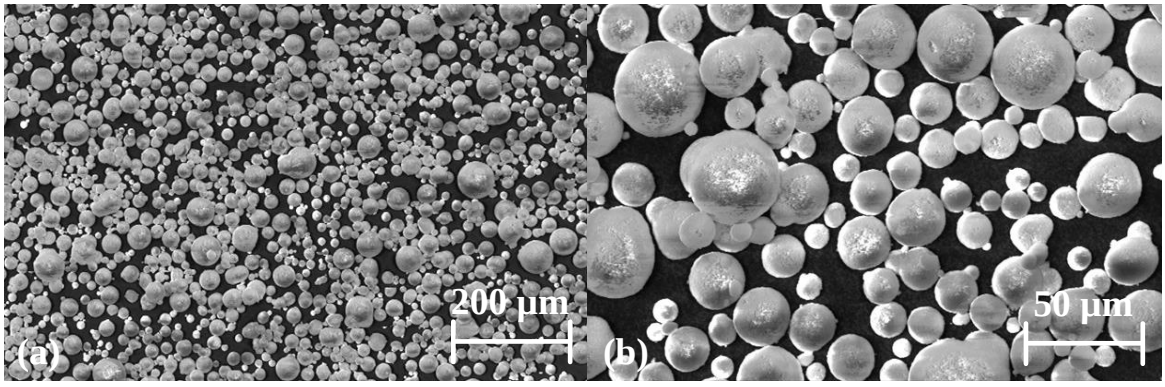


***Figure 4.17*** *Morphology of the spray-dried granules from the suspension with 45 wt% alumina (0.6 µm), 2 wt% binder, 0.5 wt% lubricant, 0.195 vol.% GO and 0.3 wt% dispersant.*

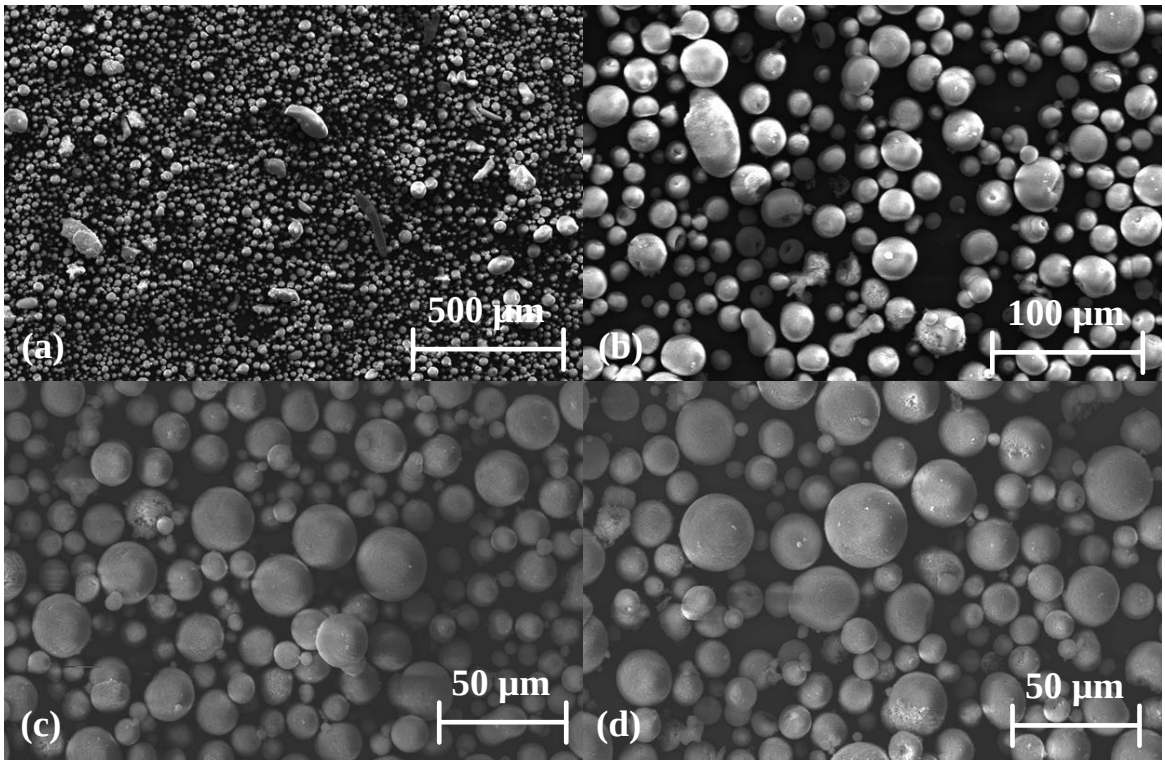


***Figure 4.18*** *Morphology of the spray-dried granules from the suspension with 2 wt% binder, 0.5 wt% lubricant, 0.065 vol.% GO, (a, b) 55 wt% alumina (0.3 µm) and 0.4 wt% dispersant, (c, d) 50 wt% alumina (0.3 µm) and 0.3 wt% dispersant.*

### HH300-065 and HH300-195

In order to formulate the HH300-065 suspension, two different suspensions with different formulations were prepared. The first suspension was prepared by using 55 wt% solid content and 0.4 wt% dispersant whereas the second suspension consisted of 50 wt% solid content and 0.3 wt% dispersant. The morphology of the spray-dried granules is shown in Figure 4.18 . As it can be seen, huge rod-shaped structures can be found among the granules obtained from the first suspension (Figure 4.18 (a)) which indicates high amount of solid content. In addition to that, most of the granules have blow holes on their external surface and also some donut-shaped structures which can be found in Figure 4.18 (b). On the other hand, the spray dried granules obtained from the second suspension had solid spherical morphology (Figure 4.18 (c, d)) which indicates that reducing the amount of dispersant from 0.4 wt% to 0.3 wt% makes the suspension slightly flocculated and therefore solid spherical granules are formed. The finalized formulation of the HH300-065 suspension can be found in Table 4.8.

In order to formulate the HH300-195, solid content was reduced to 40 wt%. The

***Table 4.8*** *Formulation of the HH300-065 suspension.*

| Suspension | $Al_2O_3$ (wt%) | Dispersant (wt%) | Binder (wt%) | Lubricant (wt%) | GO (vol.%) |
|---|---|---|---|---|---|
| **HH300-065** | 50 | 0.3 | 2 | 0.5 | 0.065 |

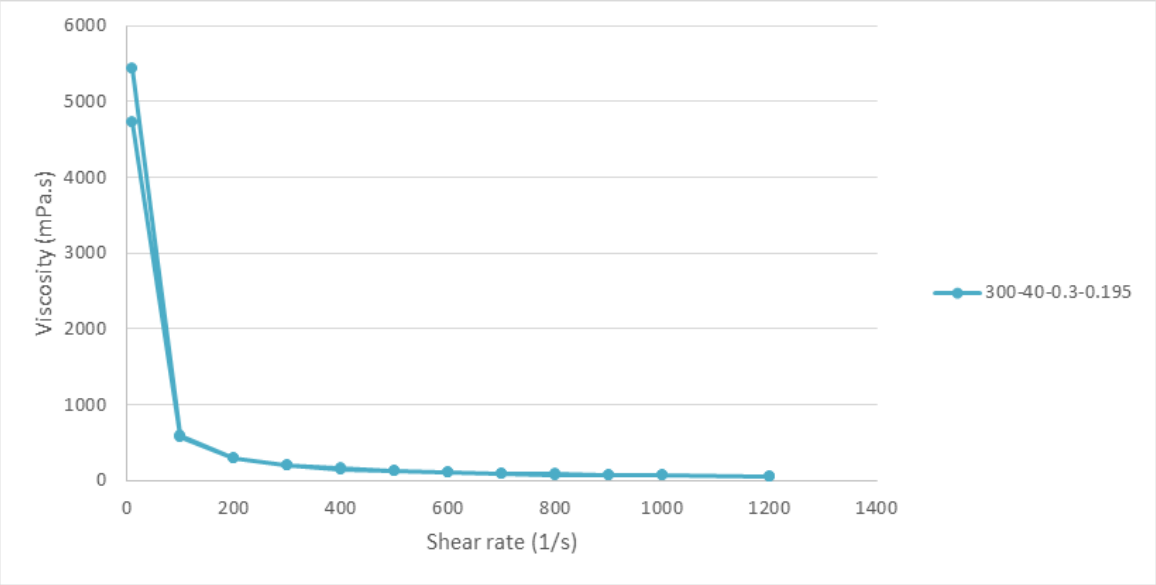


***Figure 4.19*** *Viscosity of the suspension with 40 wt% alumina (0.3 µm), 2 wt% binder, 0.5 wt% lubricant, 0.3 wt% dispersant and 0.195 vol.% GO.*

prepared suspension was thick due to the significant bridging effect of GO and therefore, spray drying was difficult as the hose was blocked many times with the suspension. The viscosity of the prepared the suspension is depicted in Figure 4.19 which shows high viscosity of the suspension ($\sim$ 4730 mPa.s) at low shear rate (10 $s^{-1}$), indicating the presence of continuous chains of alumina particles produced by the bridging effect of GO sheets. However, viscosity reached to $\sim$ 56 mPa.s at the shear rate of 1200 $s^{-1}$. The solid spherical granules obtained from spray drying this suspension and the finalized formulation of the HH300-195 suspension is shown in Figure 4.20 and Table 4.9, respectively.

***Table 4.9*** *Formulation of the HH300-195 suspension.*

| Suspension | $Al_2O_3$ (wt%) | Dispersant (wt%) | Binder (wt%) | Lubricant (wt%) | GO (vol.%) |
|---|---|---|---|---|---|
| **HH300-195** | 40 | 0.3 | 2 | 0.5 | 0.195 |

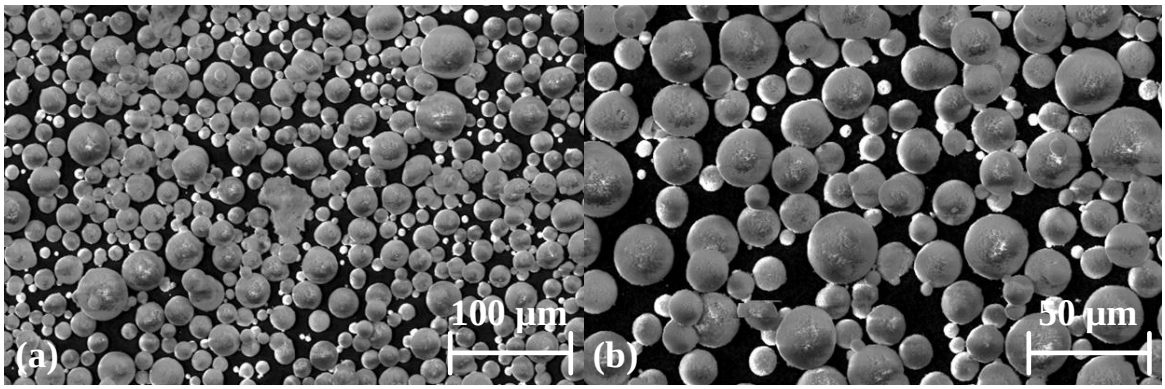


***Figure 4.20*** *Morphology of the spray-dried granules from the suspension with 40 wt% alumina (0.3 µm), 2 wt% binder, 0.5 wt% lubricant, 0.195 vol.% GO and 0.3 wt% dispersant.*

### 4.2.3 SEM characterization of the internal structure of the spray-dried granules

Figure 4.21 shows the internal structure of the spray-dried granules obtained from the un-doped suspensions. As it is depicted, the granules have solid internal structures without any shell/crust or large central voids. However, very small few holes can be observed in their internal structure of the granules which are probably due to the bubble formation. Bubbles were formed during the thermal equilibrium with the heated gas air. When the temperature exceeds the boiling point of water, the pressure of the moisture vapor inside the droplet will be higher than the ambient pressure, leading to the formation of bubbles. Moreover, as it can be seen, the ground cross-sectional surface of the granules is porous since water has to diffuse through these paths. According to Figure 4.21 (a, d), the cross-sectional surface of the granules obtained from the submicron sized primary particles are more uniform and even compared to the surface of the granules obtained from the micron sized primary particles which is probably due to their finer particle size of 0.3 and 0.6 $\mu$m powders.

The internal structures of the granules obtained from the alumina suspensions doped with 0.065 vol.% GO is shown in Figure 4.22. As it can be seen, most of the granules have solid surface, indicating that the suspensions were slightly flocculated as water flowed without carrying the particles. However, again small holes can be seen in the internal structure of the granules which are due to the bubble formation phenomena. These holes are bigger than the holes formed in the internal structure of the granules obtained from un-doped suspensions shown in Figure 4.21. This can be explained by the presence of GO which is hydrophilic and therefore, water was trapped inside

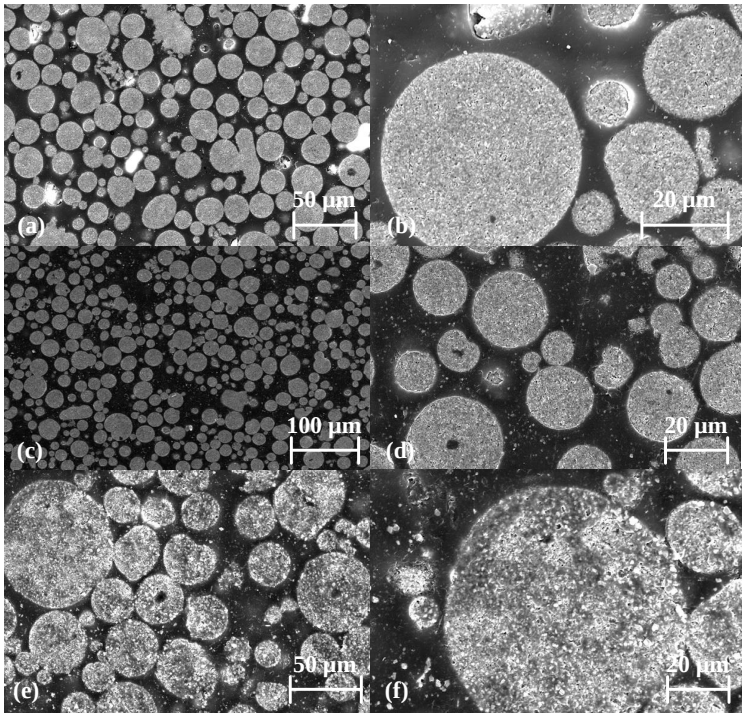


***Figure 4.21*** *Internal structure of spray-dried granules obtained from the (a, b) HH300-00, (c, d) HH600-00, (e, f) HH1000-00 suspension.*

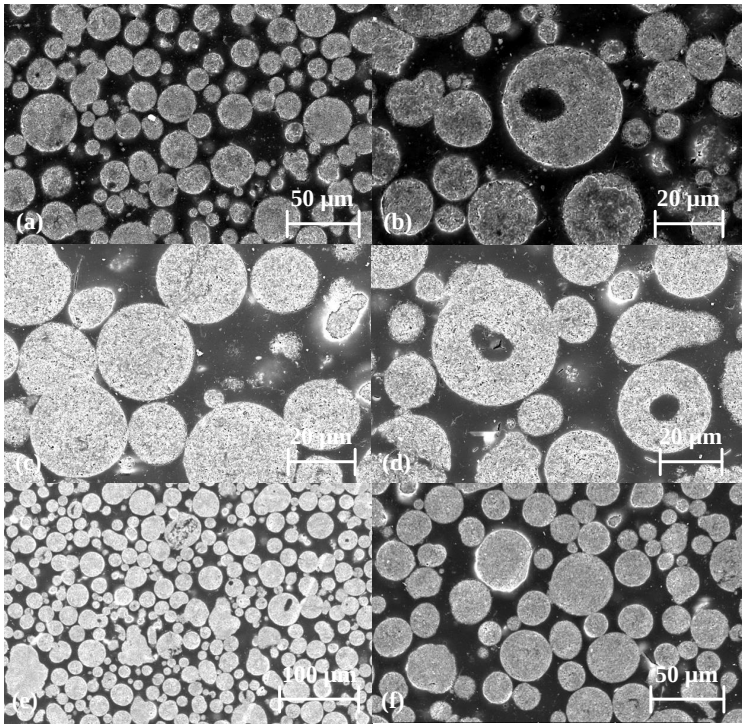


***Figure 4.22*** *Internal structure of spray-dried granules obtained from the (a, b) HH300-065, (c, d) HH600-065, (e, f) HH1000-065 suspension.*

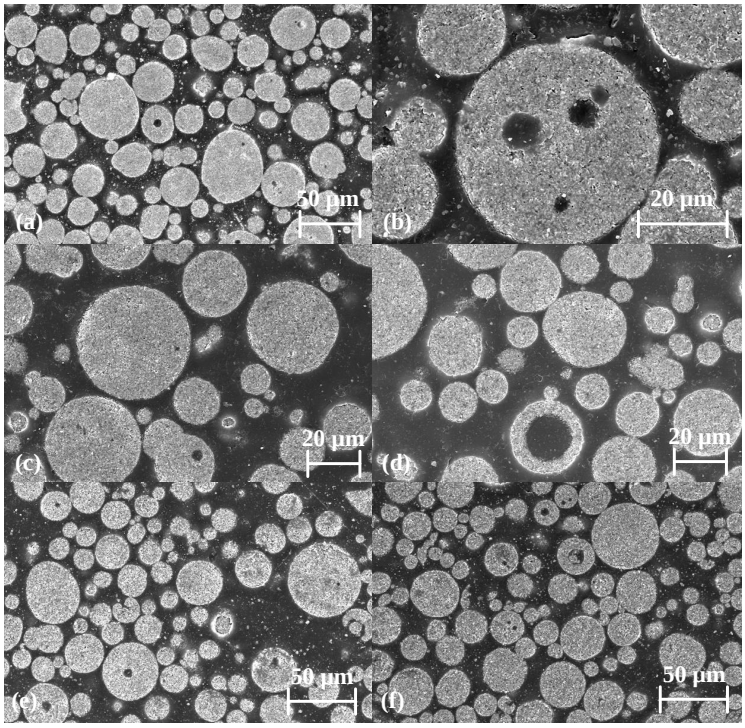


***Figure 4.23*** *Internal structure of spray-dried granules obtained from the (a, b) HH300-195, (c, d) HH600-195, (e, f) HH1000-195 suspension.*

the droplets for a longer time and led to the formation of bubbles.

The internal structures of the granules obtained from the alumina suspensions doped with 0.195 vol.% GO is shown in Figure 4.23. As it is clear from the figure, presence of more GO into the alumina matrix results in multiple small voids (Figure 4.23 (b, f)) and in some cases, one larger void (Figure 4.23 (d, f)) in a granule. This again indicates that water could not migrate easily due to the hydrophilic surface state of GO.

## 4.3 Compression curves

The compaction curves of the spray-dried granules obtained from the HH1000-00, HH1000-065 and HH1000-195 suspensions are shown in Figure 4.24. As it is shown, the granules obtained from the HH1000-00 suspension had the highest relative density of 0.80 when 10kN (33.5 MPa) force was applied for compressing the granules. However, the relative density was reduced to 0.79 and 0.76 for the the granules obtained from the HH1000-065 and HH1000-195, respectively. This result is consistent with the results obtained from the SEM characterization of the internal structure of the granules. As it was seen from Figure 4.21, all of the un-doped granules had solid structures without any shell or crust. Therefore, it is easier to fracture the un-doped

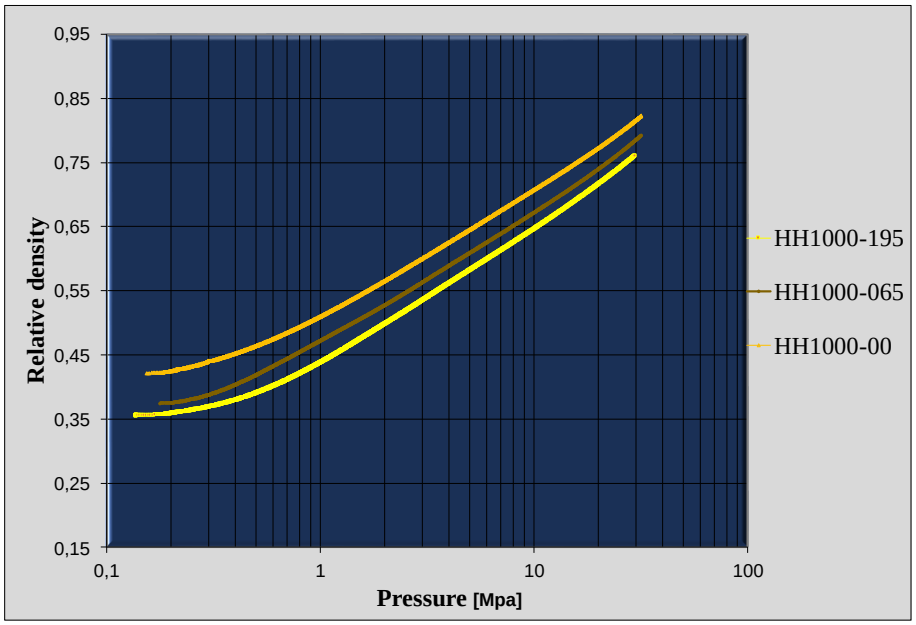


***Figure 4.24*** *Compression curve of spray-dried ganules obtained from the HH1000 suspensions.*

granules and obtain higher relative density. However, in case of the doped granules, crust structures or multiple holes could be observed in the internal structure of the granules which was due to the presence of GO and its hydrophilic surface state. Therefore, it requires more force to fracture these strong crusts. In addition to that, GO has exceptional intrinsic strength with high Young's modulus of 290-430 GPa according to the change in the coverage of the oxygen-containing groups [73]. Therefore, presence of GO into the alumina matrix hardens the external structure of the granules and it requires more force to fracture the granules and eliminate all the voids between the granules.

The same results were obtained from the compression curves of the spray-dried granules achieved from the HH600-00, HH600-065 and HH600-195 suspensions, shown in Figure 4.25 and also from the HH300-00, HH300-065 and HH300-195 suspensions, shown in Figure 4.26. The relative density of the compressed green bodies made from different spray-dried granules can be found in Table 4.10.

***Table 4.10*** *Relative density of the compressed green bodies made from different spray-dried granules with the pressure of 33.5 MPa.*

| | HH-1000 | HH-600 | HH-300 |
|---|---|---|---|
| Un-doped | 0.8066 | 0.762 | 0.78 |
| Doped by 0.065 vol.% | 0.7903 | 0.7535 | 0.7709 |
| Doped by 0.195 vol.% | 0.7674 | 0.73 | 0.7685 |

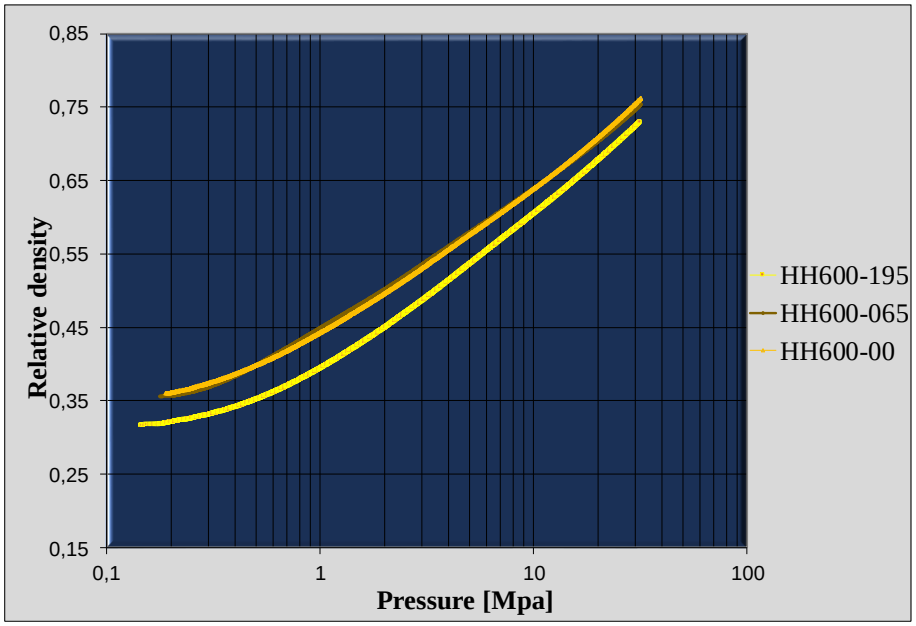


***Figure 4.25*** *Compression curve of spray-dried ganules obtained from the HH600 suspensions.*

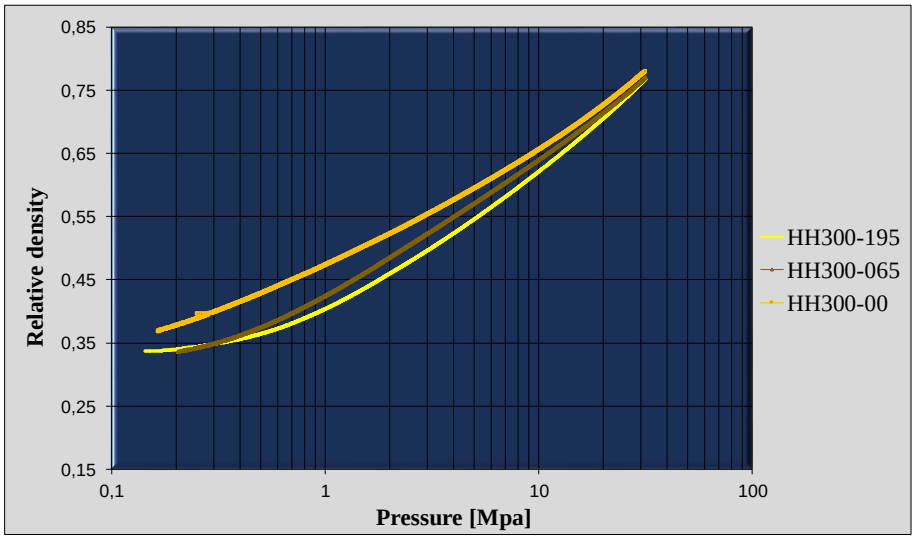


***Figure 4.26*** *Compression curve of spray-dried ganules obtained from the HH300 suspensions.*

# 5. CONCLUSION

In this thesis work, three alumina powders with the average particle size of 0.3, 0.6 and 1 $\mu$m were used. In order to achieve solid spherical granules with the highest solid content, the prepared suspensions had to be slightly flocculated. In this case, the primary particles are in contact with each other due to the van der Waals forces between them and therefore, agglomerations are found in the suspension. The presence of flocs in the colloidal suspension lets the water migrate and evaporate easily without carrying the loosely packed agglomerations as it flows towards the surface of the droplet and hence, solid structures are formed. However, the suspension should not be very flocculated as the viscosity increases by the presence of agglomerations which is not favorable for spray drying.

Spherical spray-dried granules were obtained from the HH1000-00 suspension with 70 wt% solid content, 0.3 wt% dispersant, 1.5 wt% binder and 0.3 wt% lubricant. Although, granules were spherical but some of them had craters or blow holes on the external surface of the granules. In order to achieve solid spherical granules without any craters or donut-shaped structures from the HH600-00 suspension, the amount of dispersant was reduced to 0.2 wt%. Moreover, the solid content was reduced to 60 wt% as the primary particle size is reduced from 1 $\mu$m to 0.6 $\mu$m. This was due to the fact that with this primary particle size, compared to the 1 $\mu$m powder, the separating distance between the alumina particles is reduced and therefore, more agglomerations are formed in the suspension. In addition to that, more binder and lubricant were required in order to compress the granules without any breakage of the compressed green body since the surface area is larger for this primary particle size compared to the 1 $\mu$m powder. Therefore, 2 wt% binder and 0.5 wt% lubricant were used for spray drying the HH600-00 suspension. To obtain solid spherical granules from the HH300-00 suspension, solid content had to be reduced to 55 wt% due to the fine submicron size of the primary particles. However, the same amount of additives which were used for the HH600-00 suspension, were also used for the HH300-00 suspension. The SEM images of the spray-dried granules from different formulation trials revealed the fact that any amount of dispersant more than the optimized amount resulted in donut-shaped structures whereas any amount of solid content more than the optimized amount resulted in granules with

irregular, elongated and rod-shaped structures. Therefore, it was concluded that surface charge is not dependent on the solid content. In other words, the optimized amount of dispersant for obtaining solid structures is the same for any solid content.

Addition of GO into the alumina suspensions resulted in a significant enhancement of viscosity which was due to the two main reasons. Firstly, the larger hydrodynamic volume of GO sheets, compared to the hydrodynamic volume of the alumina particles, increases the viscosity of the suspension since GO sheets are nonspherical structures with huge aspect ratio. The difference between the hydrodynamic volume of the suspended particles corresponds to the difference in energy which is required to force the solvent around and it consequently leads to an increase of viscosity. Secondly, electrostatic attraction of negatively charged GO sheets and positively charged alumina particles results in agglomeration. As a result of this attractive interaction, GO sheet with its large aspect ratio is able to wrap up partial surface of the suspended alumina particles and therefore, bridging effect is occurred. In other words, GO sheet acts as a bridge between alumina particles, meaning that the adjacent particles are linked with each other without any direct collisions. This leads to the formation of continuous networks of alumina particles which increases the local viscosity of the suspensions. Hence, reduction of solid content was required for spray drying the doped suspensions. It is evident that the solid content of all the suspensions doped with 0.195 vol.% GO had to be less than the solid content of the suspensions doped with 0.065 vol.%. This can be explained by the fact that the presence of more GO into the alumina matrix leads to more attractive interaction of GO and alumina particles and consequently more agglomerations are formed which increase the viscosity of suspensions.

In order to spray-dry the HH1000-065 and HH1000-195 suspensions, solid content was reduced from 70 wt%, which was used for the HH1000-00 suspension, to 65 wt% and 55 wt%, respectively whereas the amount of dispersant, binder and lubricant were same as the added amount for the HH1000-00 suspension. The increase of viscosity by the presence of GO sheets was not very significant for the as-received powder with the primary particle size of 1 $\mu$m. This can be explained by the fact that probably only few alumina particles were wrapped up by GO sheets as in this case both alumina particles (1 $\mu$m) and GO sheets (16 $\mu$m) have micron size dimensions. Therefore, less alumina particles are linked with each other without direct collisions and consequently less agglomerations are formed in the suspension. However, addition of GO to the suspensions prepared by the submicron sized primary particles (0.3 and 0.6 $\mu$m) increased the viscosity significantly. This is probably due to the fact that multiple alumina particles can be adsorbed on the surface of GO sheets and therefore, more particles are indirectly in contact with each other which

increases the viscosity of the suspensions dramatically. Thus, it was necessary to increase the amount of dispersant from 0.2 wt%, which was used for the HH600-00 and HH300-00 suspensions. It was seen that by using 0.4 wt% dispersant, granules had donut-shaped structures or spherical structures with blow holes whereas by using 0.3 wt% dispersant solid spherical were achieved. In order to obtain solid spherical granules from the HH600-065 and HH600-195 suspensions, solid content was optimized to be 55 and 45 wt% whereas for the HH300-065 and HH300-195 suspensions it was optimized to be 50 and 40 wt%, respectively.

In a nut shell, addition of GO to the suspensions prepared by submicron sized powders increase the viscosity significantly and as a result, solid content had to be reduced. This is not very economical, especially in large scale production of the spray-dried GO-alumina granules, as the graphene oxide solution is very expensive. Therefore, the use of alumina powders with the micron sized primary particles for the preparation of GO doped suspensions can be recommended. The compressed green bodies made from the doped granules had less relative density compared to the compressed green bodies made from the un-doped granules. This can be explained by the presence of GO which has high intrinsic strength and therefore more force is required to fracture the granules. In addition to that, the crust structure of the spray-dried granules obtained from the doped suspension could be a reason for this result. As the amount of doping agent was increased, the relative density decreased.

# BIBLIOGRAPHY

[1] M.W.Woo, A.S. Mujumdar and W.R.W. Daud, "Spray Drying Technology", Published in Singapore, 2010.

[2] C. Anandharamakrishnan and P. I. S.,"Spray Drying Techniques for Food Ingredient Encapsulation ", *John Wiley & Sons*, 2015.

[3] R. P. Patel , M. P. Patel and A. M. Suthar, "Spray Drying Technology: an overview", Indian Journal of Science & Technology, 2(10):44-47, January 2009.

[4] A. A. Santos, I. C. Cosentino and L. A. Genova, "Evaluation of compaction behaviour of spray-dried alumina by Hg porosimetry and SEM", Materials Science Forum Vols. 727-728 (2012) pp 740-745, 2012.

[5] S. Cottrino, Y. Jorand, J. Adrien and C. Olagnon,"Spray-drying of highly concentrated nano alumina dispersions ", *Powder Technology*, 237, 568-593, 2013. http://doi.org/10.1016/j.powtec.2012.12.058

[6] O. B. Christiansen, "Successful Spray Drying", Ceramic Industry, Vol. 152, Issue 6, p60, June 2002.

[7] J. Liu, H. Yan and K. Jiang,"Mechanical properties of graphene platelet-reinforced alumina ceramic composites ", *Ceramics International*, 39(6), 6215-6221, 2013. http://doi.org/10.1016/j.ceramint.2013.01.041

[8] Y. Tamura, B. M. Moshtaghioun, D. Gomez-Garcia and A. D. Rodriguez, "Spark plasma sintering of fine-grained alumina ceramics reinforced with alumina whiskers", *Ceramics International*, 2016. http://dx.doi.org/10.1016/j.ceramint.2016.09.210

[9] L. Jianchang, Z. Xiangqiong, R. Tianhui and H. Emile van der, "The Preparation of Graphene Oxide and Its Derivatives and Their Application in Bio-Tribological Systems", *Lubricants*, 2, 137-161, 2014. doi:10.3390/lubricants2030137

[10] JJ. Swab, "Low temperature degradation of Y-TZP materials", *J Mater Sci*, Vol. 26, 6706-6714, 1991.

[11] T. Shirai, H. Watanabe, M. Fuji and M. Takahashi," Structural Properties and Surface Characteristics on Aluminum Oxide Powders", 9, 23-31, 2009.

[12] E. Dorre, H. Hubner, "Alumina-Processing Properties and Applications", *Berlin: Springer-Verlag*, p. 1-267, 1984.

[13] G. Messing and M. Kumagai, "Low Temperature Sintering of a.-Alumina Seeded Boehmite Gel", *American Ceramic Society Bulletin*, 73, No: 10, 88-91, 1994.

[14] J. S. Reed," Principles of Ceramic Processing (2nd ed.)", *New York: Wiley.*, 1995.

[15] W. D. Richardson, "Modern Ceramic Engineering, Properties, Processing and Use in Design", *2"d edition, Marcel Dekker*, 1992.

[16] Y. T. O, S. W. Kim and D. C. Shin, " Fabrication and synthesis of ?-alumina nanopowders by thermal decomposition of ammonium aluminum carbonate hydroxide (AACH)", *Colloids and Surfaces A: Physicochemical and Engineering Aspects*, 313-314, 415-418, 2008. http://doi.org/10.1016/j.colsurfa.2007.04.123

[17] H. O. Pierson, "Handbook of Carbon, Graphite, Diamonds and Fullerenes", 1994.

[18] `http://chemistrycarbons.blogspot.fi/2012/11/explanation-on-structure-of-graphite.html`

[19] H. P. Boehm, R. Setton, and E. Stumpp, "Nomenclature and terminology of graphite intercalation compounds", *Pure Appl. Chem.*, 66, 1994.

[20] K. S. Novoselov, A. K. Geim, S. V. Morozov, D. Jiang, Y. Zhang, S. V. Dubonos, I. V. Grigorieva and A. A. Firsov, "Electric field effect in atomically thin carbon films", Science, 306, 666-669, 2004.

[21] Y. Zhu, S. Murali, W. Cai, X. Li, J. W. Suk, J. R. Potts and R. S. Ruoff, "Graphene and Graphene oxide: Synthesis, properties", *Adv Mater.*, 22, 3906-3924, 2010.

[22] H. Porwal, P. Tatarko, S. Grasso, J. Khaliq, I. Dlouhý and M. J. Reece, "Graphene reinforced alumina nano-composites", *Carbon*, 64, 359-369, 2013. http://doi.org/10.1016/j.carbon.2013.07.086

[23] K. Jong-Young, S. Jae-Ho, K. Hyo-Jin, K. Ungsoo, P. Jae-Hwan, C. Woo-seok and K. J. K., "Synthesis and Characterization of graphene-alumina nanocomposite", *In 15th european conference on composite materials*, Venice, 2012.

[24] H. J. Kim, S. M. Lee, Y. S. Oh, Y. H. Yang, Y. S. Lim, D. H. Yoon and R. S. Ruoff, "Unoxidized graphene/alumina nanocomposite: fracture- and wear-resistance effects of graphene on alumina matrix", *Scientific Reports*, 4, 2014. http://doi.org/10.1038/srep05176

[25] Y. F. Chen, J. Q. Bi, C. L. Yin and G. L. You, "Microstructure and fracture toughness of graphene nanosheets/alumina composites", *Ceramics International*, 40(9 PART A), 13883-13889, 2014. http://doi.org/10.1016/j.ceramint.2014.05.107

[26] Z. Yu, H. Di, Y. Ma, L. Lv, Y. Pan, C. Zhang and Y. He, "Fabrication of graphene oxide-alumina hybrids to reinforce the anti-corrosion performance of composite epoxy coatings", *Applied Surface Sciene*, 351, 986-996, 2015. http://doi.org/10.1016/j.apsusc.2015.06.026

[27] X. Q. Cao, R. Vassen, S. Schwartz, W. Jungen and F. Tietz," Spray-drying of ceramics for plasma-spray coating", *Spray-drying of ceramics for plasma-spray coating*, 20, 0-6, 2000.

[28] M. M. Hantel, "Graphite Oxide and Graphene Oxide Based Electrode Materials for Electrochemical Double Layer Capacitors", *Technische Universität München (TUM).*, 2013.

[29] D. R. Daniel, S. Park, C. W. B. and R. S. Ruoff, "The chemistry of graphene oxide", *Chemical Society Reviews*, 39, 228-240, 2010.

[30] M. J. Readey and F. M. Mathony ,"Compaction of spray-dried ceramic powders: An experimental study of the factors that control green density", *27. international technical conference of the Society for the Advancement of Material and Process Engineering* , 9-12 Oct 1995

[31] K. Suwunnasung and A. Nuntiya," Influence of Suspension Characteristics on the Morphology of 3Y-ZrO2 Granules Produced by a Spray Drying Process", *Chiang Mai Journal of Science, an international journal for the publication of all preliminary communications in Science*, 36(3), 340-348, 2009.

[32] C. Filiatre, G. Bertrand, C. Coddet and A. Foissy,"Alumina slurry formulation intender for spray-dried powder production ", *Polymer International*, 52(4), 586-589, 2003. http://doi.org/10.1002/pi.1006

[33] G. Bertrand, P. Roy, C. Filiatre and C. Coddet, "Spray-dried ceramic powders: A quantitative correlation between slurry characteristics and shapes of the granules", *Chemical Engineering Science*, 60(1), 95-102, 2005. http://doi.org/10.1016/j.ces.2004.04.042

[34] W. Liu, X. D. Chen and C. Selomulya ," Particuology On the spray drying of uniform functional microparticles", *Particuology* 22, 1-12, 2015. http://doi.org/10.1016/j.partic.2015.04.001

[35] K. Masters," Spray drying handbook. Essex", *UK: Longman Scientific & Technical*, 1985.

[36] S. Keshani, W. Ramli, W. Duad, M. M. Nourouzi, F. Namvar and M. Ghasemi,"Spray drying: An overview on wall deposition, process and modeling ", *Journal of Food Engineering*, 146, 152-162, 2015. http://doi.org/10.1016/j.jfoodeng.2014.09.004

[37] A. M Buergermeister and D. Reutlingen,"Droplet Sizes and Droplet Spectrums of Spray Dry Nozzles and Rotary Atomizers under typical conditions of use", *European Conference on Liquid Atomization and Spray Systems*, 8-10, 2008.

[38] S. J. Lukasiewicz , "Spray-Drying Ceramic Powders ", *Journal of the American Ceramic Society*, 72(4), 617-624, 1989.

[39] K. Murali, S. M. Kannan, M. S, Prabhu, S. K. Sk, B. Aathutha, N. Ashok and P. Jeya, " Correlation Development for Sauter Mean Diameter of Rotary Atomizer", (3), 339-345, 2014.

[40] E. Teunou and D. Poncelet ," Rotary disc atomisation for microencapsulation applications - prediction of the particle trajectories", 71, 345-353, 2005. http://doi.org/10.1016/j.jfoodeng.2004.10.048

[41] A. Sosnik and K. P. Seremeta , "Advantages and challenges of the spray-drying technology for the production of pure drug particles and drug-loaded polymeric carriers", *Advances in Colloid and Interface Science*, 223, 40-54, 2015. http://doi.org/10.1016/j.cis.2015.05.003

[42] W. Julklang and B. Golman, "Effect of process parameters on energy performance of spray drying with exhaust air heat recovery for production of high value particles", *Applied Energy*, 151, 285-295, 2015. http://doi.org/10.1016/j.apenergy.2015.04.069

[43] M. Mezhericher, A. Levy and I. Borde," Modelling the morphological evolution of nanosuspension droplet in constant-rate drying stage", *Chemical Engineering Science*, 66(5), 884-896, 2011. http://doi.org/10.1016/j.ces.2010.11.028

[44] M. Michálková, M. Michálek, D. Galusek, G. Blugan, J. Kuebler and P. Ś., "Separation of CNF agglomerates from a ceramic suspension by spray drying technique", 42, 15787-15792, 2016. http://doi.org/10.1016/j.ceramint.2016.07.044

[45] H. Abe, M. Naito, T. Hotta, H, Kamiya and K. Uematsu, "Pore defects related to slurry character and their relevance to strength distribution in alumina ceramics", *Powder Technology*, 134(1-2), 58-64, 2003. http://doi.org/10.1016/S0032-5910(03)00127-X

[46] D. Kim and J. Jung, "Granule performance of zirconia / alumina composite powders spray-dried using polyvinyl pyrrolidone binder", *Journal of the European Ceramic Society*, 27, 3177-3182, 2007. http://doi.org/10.1016/j.jeurceramsoc.2007.01.013

[47] M. Goli, A. Sharifi, M. Y. Jozdani and S. A. M.," Effects of Spray Dryer Atomizer Speed on Casein Micelle Size in Whole Fat Milk Powder and Physicochemical Properties of White Cheese", *In ICFPE 2015?: 18th International Conference on Food Process Engineering* , Vol. 2, 2015.

[48] A. H. Bahnasawy, A. E. Okasha and E. E. G., "PERFORMANCE EVALUATION OF A LABORATORY SCALE SPRAY DRYER", *Misr Journal of Agricultural Engineering*, 27(1), 326-346, 2010.

[49] E. Esposito, R. Roncarati and R. Cortesi, "Production of Eudragit microparticles by spray-drying technique: influence of experimental parameters on morphological and dimensional characteristics", *Pharm. Dev. Technol.*, 5, 267-278, 2005.

[50] A. L. R. Rattes and W. P. Oliveira, "Spray drying conditions and encapsulating composition effects on formation and properties of sodium diclofenac microparticles", *Powder Technol.*, 171, 7-14, 2007.

[51] V. Paramita, K. Lida, H. Yoshii and T. Furuta, "Effect of additives on the morphology of spray-dried powder", *Drying Technol.*, 28, 323-329, 2010.

[52] S. G. Mass, G. Schaldach and E. M. Littringer, "The impact of spray drying outlet temperature on the particle morphology of mannitol", *Powder Technol.*, 213, 27-35, 2011.

[53] K. Sarabandi, S. H. Peighambardoust and M. S."Physical properties of spray-dried grape syrup as affected by drying temperature and drying aids ", *International Journal of Agriculture and Crop Sciences*, 7(12), 928-934, 2014.

[54] S. Chiangka, S. Watcharamaisakul and B. G.,"Effect of Slurry Formulation on Morphology and Flowability of Spray-Dried Alumina / Zirconia Composite Particles ", *Key Engineering Material*, 675-676(March), 531-534, 2016. http://doi.org/10.4028/www.scientific.net/KEM.675-676.531

[55] P. Penbunditkul, H. Yoshii, U. Ruktanonchai, T. Charinpanitkul and A. Soottitantawat, "Effect of feed liquid viscosity on flavor retention of bergamot oil encapsulated in spray-dried modified starch powder", *In International Congress on Engineering and Food*, Athens, Greece, 2011.

[56] H. min Bian, Y. Yang, Y. Wang and W. Tian, "Preparation of nanostructured alumina-titania composite powders by spray drying, heat treatment and plasma treatment", *Powder Technology*, 219, 257-263, 2012. http://doi.org/10.1016/j.powtec.2011.12.055

[57] E. Sanchez, A. Moreno, M. Vicent, M. D. Salvador, V. Bonache, E. Klyatskina and R. Moreno," Preparation and spray drying of Al2O3-TiO2 nanoparticle suspensions to obtain nanostructured coatings by APS", *Surface and Coatings Technology*, 205(4), 987-992, 2010. http://doi.org/10.1016/j.surfcoat.2010.06.002

[58] M. V. A. Umaran and R. L. Menchavez," Aqueous Dispersion of Red Clay-based Ceramic Powder with the Addition of Starch", *Materials Research*, 16(2), 375-384, 2013. http://doi.org/10.1590/S1516-14392013005000002

[59] B. Patel Bhavesh, K. Patel Jayvadan, C. Subhashis and S. D., "Revealing facts behind spray-dried solid dispersion technology used for solubility enhancement", *Saudi Pharmaceutical Journal*, 23, 352-365, 2015.

[60] B. P. Singh, S. Bhattacharjee and L. Besra ," Influence of surface charge on maximizing solids loading in colloidal processing of alumina", *Materials Letters* 56(October), 475-480, 2002.

[61] X. Wang, R. Wang, C. Peng and H. Li," Rheology of aqueous BeO suspension with NH 4 PAA as a dispersant", *Progress in Natural Science: Materials International*, 22(4), 347-353, 2012. http://doi.org/10.1016/j.pnsc.2012.07.003

[62] H. Sarraf and J. Havrda," RHEOLOGICAL BEHAVIOR OF CONCENTRATED ALUMINA SUSPENSION: EFFECT OF ELECTROSTERIC STABILIZATION", *Ceramics Silikáty*, 51, 147-152, 2007.

[63] P. P. Nampi, S. Kume, Y. Hotta, K. Watari, M. Itoh, H. Toda and A. Matsutani," The effect of polyvinyl alcohol as a binder and stearic acid as an internal lubricant in the formation, and subsequent sintering of spray-dried alumina", *Ceramics International*, 37(8), 3445-3450, 2011. http://doi.org/10.1016/j.ceramint.2011.05.149

[64] S. Balasubramanian, D. J. Shanefield and D. E. Niesz, "Effect of Internal Lubricants on Defects in Compacts Made from Spray-Dried Powders", *Journal of the American Ceramic Society*, 85(1), 134-138, 2002.

[65] D. Sharma and A. Mukherjee," Essential parameters responsible for rheological assessment of concentrated dispersion: a comprehensive review", *Journal of Ceramic Processing Research*, 16(6), 690-740, 2015.

[66] P. Ramavath, R. Papitha, M. Ramesh, P. Babu and R. Johnson," Effect of primary particle size on spray formation, morphology and internal structure of alumina granules and elucidation of flowability and compaction behaviour", *Processing and Application of Ceramics*, 8(2), 93-99, 2014. http://doi.org/10.2298/PAC1402093R

[67] S. Eckhard, M. Fries, S. Höhn and C. Rödel," Influence of varied suspension properties on properties of spray-dried granules", *In 12th Triennial International Conference on Liquid Atomization and Spray Systems*, pp. 1-8, Heidelberg, Germany,2012.

[68] K. Somton, K. Dateraksa, D. Atong and R. Mccuiston, "The Effect of Granule Morphology and Composition on the Compaction Behavior and Mechanical Properties of 92 % Alumina Spray Dried Granules", 22(2), 41-47, 2012.

[69] Lin Ching-Shan and L. S.-T., "Effects of granule size and distribution on the cold isostatic pressed alumina", *Journal of Materials Processing Technology*, 201(1-3), 657-661, 2008.

[70] R. D. Carneim, "Characterization of uniaxial compaction in spray dried ceramic powders", USA 2000, The Pennsylvania State University, A thesis in Material Science and Engineering.

[71] R. B. Langston and J. A. Pask, "Analysis of consistencies of kaolin-water systems below the plastic range", 1956.

[72] Y. Yao, X. Zeng, R. Sun and J. Xu, "Study on the bridge effect of graphene oxide on thermal conductivity of Al2O3 filled glass fibers reinforced polymer composites", Electronic Packaging Technology (ICEPT), 2014 15th International Conference on, Chengdu, pp. 296-300, 2014. doi: 10.1109/ICEPT.2014.6922658

[73] L. Liu, J. Zhang, J. Zhao and F. Liu, "Mechanical properties of graphene oxides", 2012. DOI: 10.1039/C2NR31164J